Institut für Veterinärbiochemie und Molekularbiologie
der Vetsuisse-Fakultät Universität Zürich

Direktor: Prof. Ulrich Hübscher

Interface between science and art: Can art predict functions of enzymes?

Inaugural-Dissertation

zur Erlangung der Doktorwürde der
Vetsuisse-Fakultät Universität Zürich

vorgelegt von

Céline Clemenz

cand. med. vet.
von Stalden-Staldenried, VS

genehmigt auf Antrag von
Prof. Ulrich Hübscher, Referent
Prof. Hanspeter Nägeli, Korreferent

Zürich 2009

1. Summary

1.1 English

The aim of this study was to scientifically verify predictions based on the „metasystem PerZan". For this purpose 20 DNA polymerase (pol) λ mutants, generated *in silico,* were analyzed by Karsten Knut Panzer with his „metasystem PerZan". According to his predictions, these 20 mutants were subdivided into five classes of mutational success, whereof four different mutants have been chosen. These pol λ mutants were produced by site-directed mutagenesis, cloned in *E. coli*, expressed and purified. They were subjected to scientific verification. Firstly, different titrations were done over a control (39/72 mer) and an 8-oxo-G lesion (39/8oxoG72 mer) primer/template. According to the titration of the mutant pol λ enzymes over these primer/templates the mutants were ranked referring to their activity and efficiency. Secondly, the same was done by titrating dNTPs. The results indicated that K312V was the most active and efficient mutant, followed by Y267W and A349P; D490K was inactive. That order was also predicted by the „metasystem PerZan". With single nucleotide titration over the same templates an other order was found, namely that the mutant A349P was better incorporating the correct dCTP than the wild type (WT), followed by Y267W, K312V and D490K. In summary, this thesis study suggested that the „metasystem PerZan" might give a valuable overview, but more work is needed to verify the „PerZan hypothesis" as a predictable way to suggest protein functions in biology and medicine.

1.2 German

Das Ziel dieser Studie war es Voraussagen, die durch das „Metasystem PerZan“ gemacht wurden, wissenschaftlich zu überprüfen. Dazu wurden 20 DNA-Polymerase (pol) λ Mutanten *in silico* generiert und von Karsten Knut Panzer mit seinem „Metasystem PerZan“ analysiert. Anhand seiner Vorhersagen wurden diese 20 pol λ Mutanten in fünf Klassen von „Mutationserfolgen” eingeteilt, wovon vier Mutanten ausgewählt wurden. Diese pol λ Mutanten dienten zur wissenschaftlichen Überprüfung. Durch gezielte Mutagenese wurden die pol λ Mutanten hergestellt, in *E. coli* kloniert, exprimiert, gereinigt und analysiert. Erstens wurden die pol λ Enzyme an einer Kontroll (39/72 mer) und einer 8-oxo-G (39/8oxoG72) Primer/Matrize titriert. Anhand der Ergebnisse wurden die pol λ Mutanten nach ihrer Aktivität und Effizienz geordnet. Zweitens wurde dasselbe gemacht für die dNTPtitration. Es zeigte sich, dass K312V die aktivste und effizienteste Mutante war, gefolgt von Y267W und A349P. D490K war inaktiv. Diese Reihenfolge wurde auch vom „Metasystem PerZan“ vorhergesagt. Mit der Einzelnukleotidtitration an denselben Primer/Matrizen wurde eine andere Reihenfolge gefunden. Die Mutante A349P baute das korrekte dCTP besser ein als der Wildtyp, gefolgt von Y267W, K312V und D490K. Zusammenfassend konnte gezeigt werden, dass das „Metasystem PerZan“ einen Überblick geben kann. Weitere Studien sind notwendig, um die „PerZan Hypothese“ als Voraussage für Proteinfunktionen in Biologie und Medizin zu etablieren.

2 Introduction

2.1 DNA stability, the cell cycle and DNA damage checkpoints

All the genetic information that enables a cell to develop, to divide and to react to its environment is stored in the DNA, which is mainly located in the cell nucleus. The maintenance of genome integrity is essential for the proper function and survival of all organisms. This task is particularly daunting due to constant assault on the DNA by endogenous and exogenous factors. DNA damage, due to environmental factors and normal metabolic processes inside the cell, occurs at a rate of 1,000 to 1,000,000 molecular lesions per cell and day (Lodish and Darnell, 1995). Sources for endogenously caused DNA damage may be firstly oxidation, for example due to reactive oxygen species (ROS) generated as normal metabolic byproducts. Secondly, spontaneous base loss due to hydrolysis of the chemically instable N-glycosilic bond and thirdly by alkylation or non-enzymatic methylation (Lindahl, 1993). Furthermore also the infidelity of certain DNA polymerases (pols) can lead to misincorporation of dNTPs during DNA replication and repair. On the other hand sources for exogenous DNA damages are for example ionizing radiation (IR), ultraviolet (UV) radiation and various chemical agents.

To guarantee survival, a cell has to be able to replicate its DNA correctly and to repair the damages, in order to maintain the sequence and structure of this crucial molecule stable and active physiological ranges over the entire lifespan. Over billions of years of evolution many different strategies have evolved in order to make a cell able to respond to those two tasks of replication and repair in the most efficient way possible. Only the most successful strategies have been conserved over this vast time span by being constantly inherited to the subsequent cell generations.

The cellular response to DNA damages may involve activation of a cell cycle checkpoint, commencement of transcriptional programs, execution of DNA repair or when the damage is severe, initiation of apoptosis.

The cell cycle is divided into the four phases: G1 (gap 1) as the phase of the cells normal activity state, followed by the S-phase (synthesis), representing the period in which the DNA is copied. Afterwards, the cell enters the G2-phase (gap 2), an important phase to enable preparation and initiation of cell division and finally the M-phase (mitosis), in which the cell divides itself in two identical daughter cells. As a fifth stage the G0-phase (gap 0), a steady equivalent of the G1-phase, represents the state of the cells that have undergone full differentiation and cannot divide further under normal circumstances.

This cell cycle progression is strongly regulated and surveyed by so called cell cycle checkpoints. By means of highly sophisticated pathways that can be activated at those checkpoints, the cell surveys the progression of every phase of the cycle, even under severe circumstances. The cellular response provoked by DNA damage consists of slowing down the cell cycle and stalling it completely at the G2/M transition (Foiani et al., 2000), to provide the necessary time to repair damage through multiple different DNA repair pathways (Christmann et al., 2003). These mechanisms include base excision repair (BER), nucleotide excision repair (NER), mismatch repair (MMR) and double-strand break repair (DSBR).

2.2 DNA repair

As mentioned above, there are several mechanisms of repair. Pol λ, which is the main focus of this study, is mainly involved in BER and NHEJ (Ramadan et al., 2004).

2.2.1 Base excision repair (BER)

Base excision repair is a multi-step process that corrects non-bulky damage to bases resulting from oxidation, methylation, deamination or spontaneous loss of the DNA base itself (Memisoglu and Samson, 2000). These alterations, although simple in nature, are highly mutagenic and therefore represent a significant threat to genome fidelity and stability (Friedberg et al., 1995).

BER consists of two sub-pathways, both of which are initiated by the action of a DNA glycosylase that cleaves the N-glycosidic bond between the damaged base and the sugar phosphate backbone of the DNA. This cleavage generates an apyrimidinic/apurinic (AP) or an abasic site in the DNA. Eight DNA glycosylases with partially overlapping base adduct specificity have been identified in humans (Maya et al., 2001). Alternatively, AP sites can also arise by the spontaneous hydrolysis of the N-glycosidic bond. In either case, the AP site is subsequently processed by AP endonuclease 1 (APE1) which cleaves the phosphodiester backbone immediately 5' to the AP site, giving rise to a 3' hydroxyl group and a transient 5' abasic deoxyribose phosphate (dRP). Removal of the dRP can amongst others be accomplished by the action of pol β, which adds one nucleotide to the 3' end of the nick and removes the dRP moiety via its associated AP lyase activity (Matsumoto and Kim, 1995). The strand nick is finally sealed by DNA ligase lll (and XRCC1), thus restoring the integrity of the DNA. Replacement of the damaged base with a single new nucleotide as described above is referred to as „short-patch" repair and represents approximately 80-90% of all BER events.

The back-up pathway of BER, termed „long-patch" repair, is employed when a modified base resistant to the AP lyase activity of pol β is present in the DNA (Matsumoto et al., 1994). Long-patch BER results in the replacement of approximately 2-10 nucleotides including the damaged base. This sub-pathway requires many of the same factors involved in short-patch repair, including a DNA glycosylase, APE1 and pol β. Unlike short-patch repair, however, long-patch repair is a PCNA-dependent pathway (Frosina et al., 1996), where the pol δ or ε add several nucleotides to the repair gap thus displacing the dRP as part of a "flap" oligonucleotide. The resulting oligonucleotide overhang is excised by the Flap endonuclease (FEN-1) prior to sealing of the nick by DNA ligase I.

2.2.2 Non-homologous end joining (NHEJ)

In addition to altered bases, DNA can also encounter double-strand breaks (DSBs), which are perhaps the most serious form of DNA damage because they pose problems for transcription, replication, and chromosome

segregation. Damage of this type is caused by a variety of sources including ionizing radiation and certain genotoxic chemicals, endogenously generated ROS, replication of single-strand DNA breaks, and mechanical stress on the chromosomes (Lindahl, 1993). DSBs differ from most other types of DNA lesions in that they affect both strands of the DNA duplex and therefore prevent use of the complementary strand as a template for repair. Failure to repair these defects can result in chromosomal instabilities leading to disregulated gene expression and carcinogenesis (Hoeijmakers, 2001). To counteract the detrimental effects of these potent lesions, cells have evolved two distinct pathways of DSBR (Jackson, 2002), namely homologous recombination (HR) and NHEJ. The cellular decision as to which pathway to utilize for DSBR is unclear, however, it appears to be largely influenced by the stage of the cell cycle at the time of damage acquisition (Takata et al., 1998). Generally HR occurs during the S-phase of the cell cycle.

NHEJ is particular in that aspect as that it does not require a homologous template for DSBR and usually results in the correction of the break in an error-prone manner. Essential to the NHEJ pathway is the activity of the Ku70/Ku80 heterodimeric protein (Featherstone and Jackson, 1999). The Ku heterodimer initiates NHEJ by binding to the free DNA ends and recruiting other NHEJ factors such as DNA-dependent protein kinase (DNA-PK), XRCC4, and DNA Ligase IV to the site of injury (Jackson, 2002). DNA-PK becomes activated upon DNA binding, and phosphorylates a number of substrates including p53, Ku, and the DNA Ligase IV cofactor XRCC4. Phosphorylation of these factors is believed to further facilitate the repair process. Because the ends of most DSBs generated by genotoxic agents are damaged and therefore unable to be directly ligated, they often have to undergo limited resection by nucleases and synthesis by pols before NHEJ can be executed. The nuclease(s) responsible for this processing remains to be determined, but strong candidates for this activity include the MRE11/Rad50/NBS1 complex (Haber, 1998; Petrini, 2000), FEN-1 (Wu et al., 1999) and the Artemis protein (Moshous et al., 2001). The final step in NHEJ repair involves ligation of the DNA ends by Ligase IV in a complex that also includes XRCC4 and Ku.

2.3 DNA polymerase λ

2.3.1 Structure and function of human DNA polymerase λ

Pols are template-directed enzymes, catalyzing phosphoryl transfer reactions (Hubscher et al., 2002). Their role lies in the synthesis of long polymers of nucleotide monophosphates, whose linear addition dictated by the sequence of the complementary template DNA strand (Kelman and O'Donnell, 1994). The structure of pols has been optimized through evolution to suit the specialized tasks that each pol faces within its environment. Among the about 20 DNA pols known in an animal cell, the one that draws the attention to this work is pol λ.

Human pol λ belongs to the family X member pols (Hubscher et al., 2002). In the last 10 years, a large number of studies have provided a wealth of structural information on five family X members. They are (i) pol β (Beard et al., 2002), (ii) terminal deoxyribonucleotidyl transferase (Delarue et al., 2002), (iii) pol λ (Ramadan et al., 2004), (iv), pol μ (Garcia-Diaz et al., 2004) and (v) the African Swine Fever virus pol X (Maciejewski et al., 2001; Showalter et al., 2001).

Pols share a common overall structure resembling a right hand with three domains: the fingers, the palm and the thumb (Steitz, 1999). The structural studies of pol β and other pols has led to a model for the catalytic cycling during polymerization: polymerization begins with DNA binding followed by dNTP binding, which might trigger a conformational change from an inactive, closed conformation to an active, open one. In this regard pol λ is special in that it also seems to exist in a closed, but active conformation, even though no dNTP is bound to the active site of the pol (Garcia-Diaz et al., 2004). In summary it seems that the active site of pol λ is different from other pols studied so far.

The 575 amino acid polypeptide of human pol λ comprises an N-terminal BRCT domain, the catalytic core and a serine-proline rich region connecting the two (Garcia-Diaz et al., 2005). The catalytic core consists of three subdomains that have been linked to the fingers (residues 328-385), the palm

(residues 386-494) and the thumb (residues 495-575) of a right hand (Steitz, 1999). The 8kDa region (residues 249-327), containing the dRP lyase activity, is situated on the 39kDa catalytic core domain (Figure 1A) on the N-terminus. Thus pol λ shares the modular organization characteristic of X family enzymes.

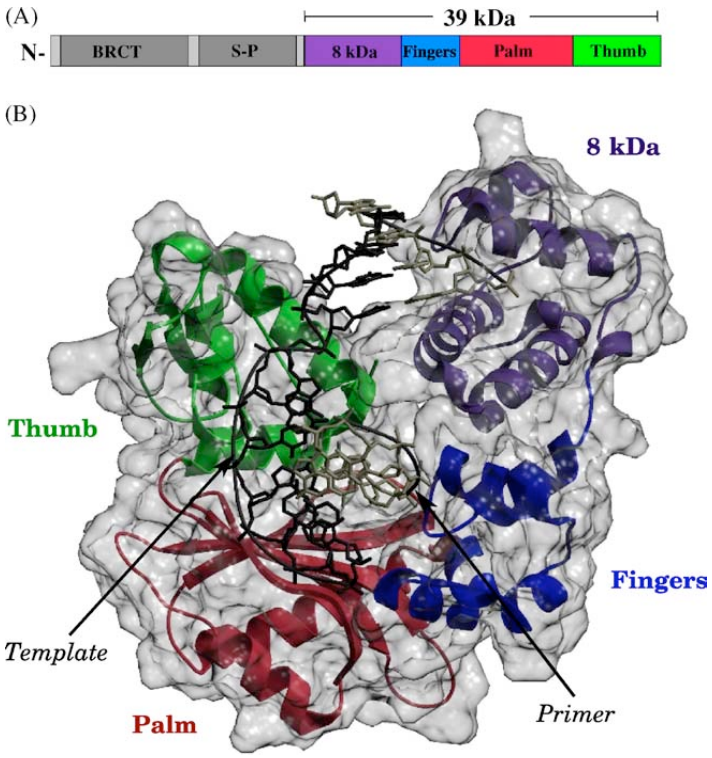

Figure 1: Domain and subdomain organization of DNA polymerase λ. A) Linear diagram indicating the different domains that compose the full-length pol λ protein: BRCT, serine-proline rich domain (S-P), 8kDa domain and the pol catalytic domain, composed of fingers, palm and thumb subdomains. **B)** Ribbon representation of the 39kDa catalytic core of pol λ in complex with a two-nucleotide gap (the DNA is shown in stick representation). The molecular surface is shown in transparent gray. The different subdomains are color coded as in A). Reproduced from (Garcia-Diaz et al., 2005).

BRCT domains are generally involved in protein-protein interactions between factors required for the cellular response to DNA damage. BRCT is associated with processing of DNA ends during NHEJ of DSBs resulting from DNA damage, and /or during V(D)J recombination (Lee et al., 2004). The serine-proline rich region connects the BRCT domain to the catalytic core (Garcia-Diaz et al., 2005) and has been suggested to be a target for

posttranslational modifications (Garcia-Diaz et al., 2000). The catalytic core is finally composed of a N-terminal 8kDa domain unique to family X pols and a pol domain, including the fingers, the palm containing the catalytic carboxylates, and the thumb subdomains that are common to all pols (Steitz, 1999). The function of the palm domain appears to be the catalysis of the phosphoryl transfer reaction whereas that of the fingers domain includes important interactions with the incoming nucleoside triphosphate as well as the template base to which it is paired. The thumb on the other hand may play a role in positioning the duplex DNA and in processivity and translocation (Steitz, 1999). The 8kDa domain includes the dRP lyase activity which can remove a 5' terminal sugar-phosphate (dRP) group (Garcia-Diaz et al., 2001). This is consistent with a possible role for pol λ in BER (Garcia-Diaz et al., 2002).

2.3.2 DNA polymerase λ and 7,8 dihydro-8-oxoguanine (8-oxo-G)

The production of ROS, such as hydrogen peroxide, superoxide and hydroxyl radicals, has been linked to the initiation and progression of cancer (Klaunig and Kamendulis, 2004). ROS are by-products of cellular respiration in mitochondria and components of inflammatory responses. In addition, ROS can be produced as a consequence of ionizing radiation or environmental exposure to transition metals, chemical oxidants and free radicals. Normal cells have enzymatic and non-enzymatic mechanisms to counteract the production of ROS. On the other hand aberrantly functioning cells are often in a state of „oxidative stress", in which the balance between oxidants and antioxidants has been disrupted, resulting in increased levels of cellular damage and thus the risk for cancer.

DNA bases are particularly susceptible to oxidation mediated by ROS (Neeley and Essigmann, 2006). The low redox potential of guanine makes this base particularly vulnerable and leads to a plethora of oxidized guanine products (Neeley and Essigmann, 2006). The most thoroughly examined guanine oxidation product is 7,8-dihydro-8-oxoguanine (8-oxo-G) (Burrows and Muller, 1998; Neeley and Essigmann, 2006). Base-excision repair plays an important role in repairing those mutations (David et al., 2007). In our laboratory it has

been shown in 2007 that pol λ might be a protection shield against these oxidative damages, since it can incorporate the correct C opposite an 8-oxo-G and thus corrects the mistakes made by the replication machinery, which often incorporates the wrong A opposite an 8-oxo-G (Maga et al., 2007). Pol λ, PCNA and RP-A together allow correct incorporation of dCTP opposite an 8-oxo-G template 1,200-fold more efficiently than the incorrect dATP. Experiments with pol-λ-null cell extracts supported this important role for pol λ (Maga et al., 2008; Maga et al., 2007). For this reason the focus of this thesis work was on pol λ and 8-oxo-G damage.

2.3.3 DNA polymerase λ in DNA repair processes

It has been well documented that the polymerase and dRP lyase activities of mammalian pol β participate in single short patch BER (Sobol and Wilson, 2001). Since pol λ can fill in short gaps, has a dRP lyase activity and can substitute or pol β in a reconstituted *in vitro* BER reaction (Sobol and Wilson, 2001) it has been proposed that pol λ may also participate in some form of BER. Support for this hypothesis comes from two studies implicating pol λ in BER (Braithwaite et al., 2005a; Braithwaite et al., 2005b).

In addition to its involvement in BER, pol λ has been implicated in NHEJ (Fan and Wu, 2004; Lee et al., 2004; Ma et al., 2004). The ability of pol λ to participate in NHEJ is clearly dependent on the presence of its BRCT domain, which enables the enzyme to interact with other end-joining proteins (Ma et al., 2005; Nick McElhinny and Ramsden, 2004; Rooney et al., 2004). However, besides this basic requirement, there is growing evidence suggesting that NHEJ pols have special properties enabling them to conduct synthesis on the non-canonical substrates that are encountered during NHEJ repair. For instance, an important feature of gap filling in the context of NHEJ may be the capacity of the pol λ 8kDa domain to bridge the gap by binding to its 5' end (Garcia-Diaz et al., 2005).

In summary pol λ appears to be involved in short-patch BER, in BER over 8-oxo-G and in NHEJ.

2.4 The „metasystem PerZan“

2.4.1 iGENE VISIONS

Science and art are in the current issue of debate often dominated by misunderstandings and the non-willingness to try to understand each other. These differences could be considered as reconciled if one were prepared to realize and evaluate the ever-increasing complexity of „worldviews” and „viewed worlds”.

In an attempt to penetrate and combine these highly complex systems, there is a need for an interdisciplinary „meta-language”, a connecting and bridging grammar of natural science and aesthetics, a general regulatory system that defines the interface between physical, biological and mental structures. The „metasystem PerZan” tries to offer such a design and uses the scientific methodology in combination with the aesthetic experience.

This synthesis-study and structural work is based on binaryly formulated representatives of two (central) culture hemispheres: on one hand on hemisphere with its western rational and biological code of the DNA and its dualism of the base pairs, A-T and G-C. On the other hand there is the eastern hemisphere with its idealistic yin-yang-polarity of the archaic „I-Ging” from the Chinese „Book of Changes”. Although the two systems hold admittedly diverse but quite possibly harmonizable items, they gradually provide instructions for an extensive transfer of knowledge between the two systems. This also means that the confrontation of between western and eastern perception and cognition almost entirely moves along with the analysis of the contrast between science and art.

The „metasystem PerZan” uses the polarity of the Chinese trigrams in which unbroken lines stand for the Yang = 0 and broken lines represent the Yin = 1 principles, thereby symbolizing the active powers of the 8 natural elements heaven, earth, fire, water, mountain, sea, thunder and wind. Out of 2 of these 8 elements, it is possible to form so-called hexagrams which are in fact the actual carriers of the information in content, and which are then used as binary reading-frames for the just as archaic but biological test of the DNA. In analogy the formal construction of the eastern system is represented by 64

components of the genetic alphabet which give rise to the 64 nucleic acids triplets which themselves are encoded by the already mentioned complementary base pairs, A-T and G-C, but also from the biochemical „binary" arrangement of purines and pyrimidines.

The project iGENE (I-Ging + Genes) VISIONS was taken up 15 years ago by Karsten Knut Panzer, a German artist, to study whether these complex structures which are identical, can also lead to a functional equalization, and if so, which regulatory system would be behind. As a mediator of such a transdisciplinary information-transmission, an unique color system with 2 integrated, three-dimensional color rooms, named „color space 64 PerZan", was developed by Karsten Knut Panzer, whose 3 main co-ordinates are the primary colors red, blue and yellow. Both, the physical color-theory as well as Goethe`s theory of colors are integrated, which, as a result, can be even confirmed from a new perspective.

Each of these 64 single cubes in the color-space 64 PerZan represents three functioning units of (i) the primary-color composed colors as a physical, (ii), a genetic amino acid as biochemical and (iii) a Chinese hexagram as a non-material functioning unit. According to the type of question and its result, the color space 64 could now function as a universal transfer- and synthesis-room.

Based on this metasystem combining genetics and art, the „metasystem PerZan" was making predictions of the „mutation success" for pol λ.

2.4.2 PerZan references

The following four references can be found in *www.perzan.de.*

www.perzan.de: Karsten K. Panzer PerZan (2001). CONSEQUENZEN

www.perzan.de: Karsten K. Panzer PerZan (2000). I GENE VISIONS

www.perzan.de: Karsten K. Panzer PerZan (1999). LIFE – CODES. VON GEIST & GENEN.

www.perzan.de: Karsten K. Panzer PerZan. WENN DIE GENE TRAUER TRAGEN.

3 Aim and project description

The aim of this study was to scientifically verify predictions made based on the „metasystem PerZan". Therefore, firstly the structure and the functions of pol λ as well as its interaction with the DNA were studied *in silico*. Taking this as a starting point, 20 different mutations in the nucleotide sequence of pol λ were proposed, which may have or may not have an influence on structure and/or function. The reason for focusing on pol λ was that this enzyme was shown in our laboratory to be 1,200 times more efficiently in incorporating a correct dCTP opposite an 8-oxo-G site in the presence of PCNA and RP-A.
The 20 pol λ mutants, generated *in silico,* were analyzed by Karsten Knut Panzer on the basis of his „metasystem PerZan". According to this, the mutants were subdivided into five classes of mutational success, whereof subsequently have been chosen four mutants of different classes. They should be subjected to scientific verification by testing them on different primer/templates, namely on a control and on an 8-oxo-G template.

Finally the obtained scientific results should be compared to the predictions made by the „metasystem PerZan".

4 Materials and methods

4.1 Buffers and solutions

$CaCl_2$ (containing 15% glycerol):

(preparation of competent cells)

100 mM $CaCl_2$

[15% (v/v) glycerol]

Resolving gel buffer for SDS PAGE:

1.5 M Tris-Base

0.4% (w/v) SDS

dissolved in ddH_20, adjusted to pH 8.8 with HCl

SDS PAGE Running buffer:

125 mM Tris-Base

1 M glycine

0.5% (w/v) SDS

dissolved in ddH_20

Stacking gel buffer:

0.5 M Tris-Base

0.5% (w/v) SDS

dissolved in ddH_20, adjusted to pH 6.8 with HCl

PCR-mix:

10 µl of 5x Phusion HF Buffer

10 mM each of dNTP, final concentration 200 µM each

10 µM of oligonucleotide primer forward

10 µM of oligonucleotide primer reverse

5 ng/µl dsDNA (pRSETb-hpol λ)

1 µl Phusion™ High-Fidelity DNA polymerase, 0.02 U/µl

ddH_2O to a final volume of 50 µl

Buffer A:

(for pol λ purification)

50 mM Tris-HCl, pH 7.5

10% (v/v) glycerol

0.05% (v/v) NP-40

1 mM PMSF

1 µg/ml pepstatin

1 µg/ml leupeptin

1 µg/ml bestatin

Buffer B:

(for pol λ purification)

50 mM Tris-HCl, pH 7.5

150 mM NaCl

10% (v/v) glycerol

0.05% (v/v) NP-40

10 mM Imidazol

1 mM PMSF

1 μg/ml pepstatin

1 μg/ml leupeptin

1 μg/ml bestatin

Buffer C:

(for pol λ purification, dialysis buffer)

20 mM Tris-HCl, pH 7.5

20% (v/v) glycerol

100mM NaCl

1 mM DTT

TBST buffer:

10 mM Tris-HCl, pH 7.5

50 mM NaCl

0.1% (v/v) Tween

Blocking buffer:

2.5% (w/v) milk powder in TBST

TBE buffer (10x):

900 mM Tris-Base

900 mM boric acid

20 mM EDTA

TBS buffer:

10 mM Tris-HCl, pH 7.5

50 mM NaCl

Lämmli buffer (2x):

500 mM Tris pH 7.5

4% (w/v) SDS

20% (v/v) glycerol

40 mM DTT

0.02% (w/v) bromphenol blue

Transfer buffer:

25 mM Tris-Base

192 mM glycine

20% (v/v) methanol

Coomassie destaining solution:
10% (v/v) acetic acid
10% (v/v) isopropanol
dissolved in H_2O

Coomassie staining solution:
10% (v/v) acetic acid
0.25% (w/v) Coomassie Blue R250
40% (v/v) methanol

Annealing buffer (5x):
100 mM Tris-HCl, pH 7.4
750 mM NaCl

S λ buffer (10x):
500 mM Tris-HCl, pH 7.5
2.5 mg/ml BSA
10 mM DTT

Stop buffer (2x):
96% formamide
20 mM EDTA, pH 8.0
bromophenol blue
xylene cyanol

4.2 Proteins

4.2.1 DNA polymerase λ, wild type

The DNA pol λ WT protein was cloned, transfected, expressed and purified according to (Wimmer et al., 2008). (For details see 4.8.)

4.2.2 DNA polymerase λ, mutants

The A349P, K312V, Y267W and D490K pol λ mutants were generated with site-directed mutagenesis according to the protocol of Garcia-Diaz (Garcia-Diaz et al., 2000). In short the DNA (dsDNA) vector with the target site for mutation was denaturated and the two oligonucleotides primers (reverse and forward), containing the desired mutation, annealed. Using the nonstrand-displacing action of DNA pol, extend and incorporate the mutagenic primers resulting in nicked circular strands. The methylated, nonmutated parenteral

DNA template was digested with Dpn1. After that the circular, nicked dsDNA was transformed in DH5α cells. The protein was generated in BL21(DE3) competent *E. coli* bacterias. The cloned protein was expressed and purified as described in (Wimmer et al., 2008). (For details see 4.8.)

4.2.3 Bovine serum albumin

Bovine serum albumin (BSA) was purchased from New England Biolabs.

4.3 Antibodies

4.3.1 His antibody selector kit

The Anti-His Antibody Selector Kit from Qiagen recognizes 4xHis-tagged proteins. The pol λ WT as well as the A349P, K312V, Y267W and D490K pol λ mutants were N-terminally 6xHis-tagged.

4.3.2 Secondary antibody

The Anti-mouse IgG was obtained from Amersham Biosciences.

4.4 DNA substrates, primers, templates

4.4.1 39/72 mer and 39/8oxoG72 mer primer/template for DNA polymerase assays

The control d72 mer, the d72 mer with the 8-oxo-G lesion and the corresponding primers were chemically synthesized and purified on denaturing polyacrylamide gel (Maga et al., 2002). The sequences are as follows:

72 mer (template):

5`-GTA TTA GAT ATT CGG GAG GTT GGG CGC CGG CGG[X/G] TGT GAA TTC GGC ACT GGC CGT CGT ATG CTC TTG GTT GTA-3`

72 mer (template) with 8-oxo-G lesion:

The position of the lesion in the undamaged template is indicated in brackets (X = 8-oxo-G).

39 mer (primer):

5`-TAC AAC CAA GAG CAT ACG ACG GCC AGT GCC GAA TTC ACA- 3`

4.5 Western blot analysis

Proteins were separated on a 12% SDS-PAGE [40% stock solution Acrylamide/Bis, solution (37.5:1), (Serva)] and electroblotted for 1.5 h at 120V (BioRad Western Blot apparatus) onto Nitrocellulose Membran (Immobilon) in transfer buffer at 4°C. After blocking the membranes for 45 min in TBST containing 2.5% powdered Milk, the membranes were incubated with the appropriate antibodies, diluted in TBST, for 2 h at room temperature. Then the membranes were washed 3 times 10 min in TBST and incubated with the corresponding secondary antibodies, diluted in TBST, for 1 h at room temperature. This was followed by washing again 3 times 10 min in TBST. The antibodies bound to the membranes were detected by Uptilight HRP blot Reagent A (Uptima) or SuperSignal West Dura Extendent Duration Substrate (Pierce).

4.6 Site-directed mutagenesis

Site-directed mutations were preformed according to the protocol of the QuikChange™ Site-Directed Mutagenesis Kit. The mutations were introduced into a human pol λ overexpression plasmid (pRSETb-hpol λ) by a PCR-based method with the following oligonucleotides: A349P-forward: 5`-GCT GGG ACC AAG ACT CCC CAG ATG TGG TAC CAA CAG; A349P-reverse: 5`-CTG TTG GTA CCA CAT CTG GGG AGT CTT GGT CCC AGC; K312V-forward: 5`-GGG AAG CGG ATG GCT GAG GTA ATC ATA GAG ATC CTG GAG; K312V-reverse: 5`-CTC CAG GAT CTC TAT GAT TAC CTC AGC CAT CGG CTT CCC; Y267W-forward: 5`-CTG GAA GTT CTG GCC AAA GCC TGG AGT GTT CAG GGA GAC AAG TGG; Y267W-reverse: 5`-CCA CTT GTC TCC CTG AAC ACT CCA GGC TTT GGC CAG AAC TTC CAG; D490K-forward: 5`-CAC CGG CGC CTG AAG ATC ATC GTG GTG CCC; D490K-reverse: 5`-GGG CAC CAC GAT GAT CTT CAG GCG CCG GTG. The first segment of the PCR was done with 98°C for 30s. The second segment was started with 98°C for 30 s, followed by 82°C (A349P), 70°C (K312V, Y267W), 68°C (D490K) for 1 min and 72°C for 1.5 min. The PCR was finished at 72°C for 5 min. The PCR products were digested with Dpn1 for 60 min at 37°C. Phusion buffer and polymerase used for PCR were from Finnzyme.

Purification of A349P, K312V, Y267W and D490K pol λ mutant plasmids was performed with NulceoBond® plasmid purification kit and sequencing done by Microsynth.

4.7 Plasmid purification

The plasmid purification was performed according to the manufactors instructions (NucleoBond® plasmid purification, high copy plasmid purification by Macherey-Nagel). The buffers S1 + RNase A, S2, S3, N2, N3 and N5 are specified in these instructions.

An overnight culture (LB medium, antibiotic, a single colony picked) was centrifuged at 6,000 x g for 15' at 4°C. The pellet was resuspended in 4 ml buffer S1 + RNase A. Afterwards 4 ml buffer S2 was added and the mixture was incubated at room temperature for 2.5 min. Further 4 ml pre-cooled buffer S3 were added and the suspension incubated on ice for 5'. At the same time the column (NucleoBond® AX 100) was equilibrated with 2.5 ml buffer N2. After that, the suspension was loaded in a filter on the column and the plasmid DNA was bound. Then the column was washed with 10 ml buffer N3 and the plasmid DNA was eluted with buffer N5 and was caught in 3.5 ml room-temperature isopropanol and centrifuged at 4,000 x g for 30' at 4°C. Further 2 ml 70% ethanol were added to the pellet, vortexed and centrifuged 4,000 x g for 15' at 4°C. The pellet was allowed to dry at room temperature for 30'. At the end the DNA pellet was dissolved in 50 μl buffer TE and stored at -20°C.

4.8 Protein purification

The purification procedure for pol λ WT and mutants was optimized in our lab (Wimmer et al., 2008).

1 l of transformed *E. coli* BL21(DE3) cells were grown at 37°C to an A_{600} of 0.6 in LB medium supplemented with 100 μg/ml ampicillin. Expression of human His-pol λ WT and mutant proteins was induced with 1 mM IPTG for 3 h and the cells were subsequently pelleted. All purification steps were carried

out at 4°C. Cells were resuspended in 60 ml buffer A supplemented with 500 mM NaCl and disrupted with a French press. Insoluble material was pelleted by centrifugation for 30 min at 48,000 g and the supernatant was diluted to a final concentration of 100 mM NaCl in buffer A. The extracts from His-pol λ WT and the four mutants were each loaded onto a 15 ml phosphocellulose column equilibrated in buffer A containing 100 mM NaCl and rolled for 2 h at 4°C. After washing with 5 ml column volume buffer A containing 100 mM NaCl, elution was performed with 60 ml buffer A containing 500 mM NaCl. The pooled eluate was diluted with an equal volume of buffer B and adjusted to 10 mM imidazol. 0.5 volumes were loaded onto a 1 ml HisTrap™ HP column (GE Healthcare) equilibrated with buffer B containing 10 mM imidazol using an ÄKTApurifier™ (GE Healthcare). After washing the column with 5 ml buffer B containing 10 mM imidazol, elution was performed using a gradient from 10 to 500 mM imidazol in buffer B and fractions containing His-pol λ were pooled. The resulting pool was diluted 1:3 with buffer A and loaded onto a 1 ml HiTrap™ Heparin HP column (GE Healthcare) equilibrated in buffer A containing 50 mM KCl. The column was washed with 5 ml buffer A containing 100 mM KCl and eluted by using a gradient from 100 mM to 1 M KCl in buffer A. A final step with buffer A with 2 M KCl was performed. The fractions containing purified His-pol λ proteins were dialyzed to buffer C and pol λ WT and the mutants were stored in small aliquots in liquid nitrogen.

After the purifications the proteins were tested for purity by SDS-PAGE and for nuclease contamination (Figure 2).

4.9 Preparation of radiolabeled primer/templates

To prepare the 39/72 mer and the 39/8oxoG72 mer primer/templates, the 39 primer was labeled at its 5`end by mixing the following reagents in a reaction mix of a final volume of 20 μl:

3.6 μM 39 mer primer (Microsynth AG)

20 μCi [γ-32P] dATP (Amersham Biosciences)

20 μl 10 x PNK buffer (New England Biolabs)

0.6 μl T4 polynucleotide kinase, 10 U/μl (New England Biolabs)

The mix was incubated for 40 min at 37°C, the kinase inactivated for 10 min at 80°C and the mix centrifuged through a G-25 (Microspin TM) column at 720 x g for 2 min to remove the free ATP. The reaction was added to the annealing mix containing following reagents to a final volume of 36 μl:

3.6 μM 72 mer or 8oxoG72 mer template (Purimex GmbH)

7.2 μl 5 x annealing buffer

This mix was heated 95°C for 10 min and slowly cooled down to room temperature over night to allow the primer to anneal to the template.

4.10 DNA polymerase assay

The DNA polymerase reaction was performed in a final volume of 10 μl containing:

50 mM Tris, pH 7.5

250 μg/ml BSA

1 mM DTT

0.8 mM $MnCl_2$

0.5 μM each of the four dNTP`s (Roche)

20 fmol 5`labeled 39*/72 mer or 39*/8oxoG72 mer primer/template and pol λ WT and mutants to be tested.

The reaction was started by adding 9 μl of the reaction mix to pol λ dilutions done in 1 μl and then incubated at 37°C for 15 min. Finally, 10 μl of 2 x stop buffer was added to each reaction tube and the reaction was put on ice. The samples were heated for 3 min at 95°C and loaded on to a 10% denaturing polyacrylamide [Acrylamide/Bis-acrylamide, 19:1 mixture, 40% (w/v)

(Qbiogene)] sequencing gel containing 7 M urea. The gels run on 100 watt, 50mA and 2500 V for 2.5 h. The result was visualized by exposing the gel to a X-ray film (Contatyp, Typon Imaging AG) overnight at -80°C, using a radioactivity-sensitivity screen (Okamoto). The quantification was done with Adobe Photoshop CS3.

The DNA polymerase reaction with different concentration of dNTP`s was performed in a final volume of 10 μl containing:

50 mM Tris, pH 7.5
250 μg/ml BSA
1 mM DTT
0.8 mM $MnCl_2$
5 ng pol λ WT or 10 ng pol λ mutants
20 fmol 5`labeled 39*/72 mer or 39*/8oxoG72 mer primer/template and the dNTP's to be tested.

The reaction was started by adding 9 μl of the reaction mix to dNTP dilutions done in 1 μl. Then the protocol described above was followed.

The DNA polymerase reaction with different concentrations of dCTP`s or dATP`s was performed in a final volume of 10 μl containing:

50 mM Tris, pH 7.5
250 μg/ml BSA
1 mM DTT
0.8 mM $MnCl_2$
2.5 ng pol λ WT or 5 ng pol λ mutants
20 fmol 5`labeled 39*/72 mer or 39*/8oxoG72 mer primer/template and dCTP or dATP to be tested.

The reaction was started by adding 9 μl of the reaction mix to dCTP of dATP solutions done in 1 μl. Then the protocol described above was followed, except that a 15%, instead of a 10%, denaturing polyacrylamide [Acrylamide/Bis-acrylamide, 19:1 mixture, 40% (w/v) (Qbiogene)] sequencing gel containing 7 M urea was used. The gels run again on 100 watt, 50mA and 2500 V but for 4 h.

4.11 Nuclease assay

The DNA nuclease assay was performed in a final volume of 10 μl containing:

50 mM Tris, pH 7.5

250 μg/ml BSA

1 mM DTT

0.8 mM $MnCl_2$

20 fmol 5`labeled 39*/72 mer or 39*/8oxoG72 mer

and pol λ WT and mutants to be tested.

The reaction, the reaction stop, the loading and the visualizing were done in the same way as the DNA polymerase assay. (For details see 4.10.)

5 Results

5.1 Rationale to design in silico mutants of DNA polymerase λ

The aim of this study was to scientifically verify predictions made based on the „metasystem PerZan". Therefore, the structure and function of pol λ was studied, as well as its interaction with DNA. Taking this as a starting point, the following 20 different mutations in the nucleotide sequence of pol λ were proposed (see Figure 1A). None of the following mutants have been published so far. This was an important perquisite to guarantee that the „metasystem PerZan" with Karsten Knut Panzer could not compare their analysis with the already existing literature. Furthermore the argumentation made below for the 20 *in silico* mutants was not given to Karsten Knut Panzer before he made his analysis by the „metasystem PerZan".

Three mutations were done in the N-terminal of pol λ (aa 1-241) where the BRCT (aa 36-126) domain is located (Garcia-Diaz et al., 2005; Garcia-Diaz et al., 2002). This domain is likely involved in protein-protein interactions between factors required for the cellular response to DNA damage (Lee et al., 2004):

Mutation 1:	A9V
Mutation 2:	A9D
Mutation 3:	P78F

Binding of the DNA by the pol and the **8kDa (aa 242-327)** domains result in a 90° bend of the DNA duplex that causes the DNA downstream of the gap to rotate out, exposing the 3' end of the primer. The bend is facilitated by a stacking the interaction between Trp 274 and the first base of the template downstream of the gap (Garcia-Diaz et al., 2004). Therefore, this amino acid was mutated:

Mutation 4:	W274Y

The catalytic domain of pol λ makes limited contacts with the DNA duplex, only interacting with the first two base pairs upstream of the primer terminus. On the other hand pol λ makes several contacts with the DNA downstream of

the gap, mainly through the 8kDa domain and to the downstream primer. The 5’ terminal phosphate on the downstream primer is buried in a positively charged pocket that also constitutes the dRP lyase active site (Garcia-Diaz et al., 2004). The dRP lyase activity can remove a 5’ terminal sugar-phosphate (dRP) group (Garcia-Diaz et al., 2001). The next four mutations were suggested in this positively charged pocket:

Mutation 5:	R308E
Mutation 6:	K312R
Mutation 16:	R308K
Mutation 17:	R275H

Furthermore a helix-hairpin-helix (HhH) motif is located in the 8kDa domain, interacts with the backbone of the downstream primer and contains the catalytic residue (Lys 312) for the dRP lyase activity (Garcia-Diaz et al., 2004). Two mutations were proposed in this HhH:

Mutation 8:	E315P
Mutation 9:	K312V

The conformational changes of pol λ, that the enzyme likely undergoes as it binds the substrates and proceeds through a catalytic cycle, result in correct positioning of the three catalytic carboxylate residues that coordinate two divalent metal ions (Garcia-Diaz et al., 2005). These metals participate in catalysis in a manner universally utilized by pols (Steitz, 1999). The next mutation was made in one of the amino acid that carries one of these three catalytic carboxylate residues:

Mutation 19:	D490K

An other HhH motif in pol λ is conserved in the **fingers (aa 328-385)** and interacts with the primer strand. This motif is common to several DNA binding proteins and confers a sequence-independent interaction with the DNA backbone (Garcia-Diaz et al., 2004). Therefore the mutation 7 was done at the position 349:

Mutation 7:	A349P

In the binary complex of pol λ, the N-helix is in the **thumb (aa 494-575)** in a location similar to that seen in the ternary complex of pol β, suggesting that pol λ is in a closed conformation, even though no dNTP is bound to the active site of the pol (Garcia-Diaz et al., 2004). The mutation in the thumb was as follows:

Mutation 10: R517H

An interaction between Arg 420 and Lys 422 of the palm subdomain and Asp 574 of the thumb subdomain in pol λ is not **present in pol β.** This interaction could help to maintain the closed conformation of the thumb of pol λ, even when dNTP is absent (Garcia-Diaz et al., 2004). Therefore the following mutations were chosen:

Mutation 11: R420K
Mutation 12: K422D
Mutation 13: D574E

The thumb - 8kDa interaction in pol λ seems to be medicated by a contact between Trp 575 and Asn 284 not observed in pol β (Garcia-Diaz et al., 2004):

Mutation 14: W575F
Mutation 15: N284T

Interestingly, pol λ Tyr 267 hydrogen bonds to the phosphate of the 5' nucleotide. This interaction is absent in pol β and probably all other human family X enzymes. The presence of this additional interaction with the 5' phosphate might account for the differences observed between pol λ and pol β regarding processing of a short gap and strand displacement (Garcia-Diaz et al., 2004):

Mutation 18: Y267W

At last the following **blind** mutation was proposed:

Mutation 20: L161Y

5.2 Analysis of 20 DNA polymerase λ mutants by the „metasystem PerZan”

The 20 pol λ mutants generated *in silico,* as described above, were analyzed by Karsten Knut Panzer on the basis of his „metasystem PerZan”. According to this, the mutants were subdivided into 5 classes of mutational success, of which four mutants were subsequently chosen:

Table 1: 20 DNA pol λ mutants analyzed by the „metasystem PerZan”

Predictions according to the „metasystem PerZan”		DNA polymerase λ mutations
+++++	„best mutation success over 5 levels”	**K312V**[1]
++++	„extrem good mutation success over 4 levels”	A9V, A9D, W274Y, R517H, **Y267W**[1], L161Y
+++	„good mutation success over 3 levels”	P78F, R308E, N284T
++	„weak mutation success over 2 levels”	**A349P**[1], R420K
	„no mutation success”	K312R, E315P, K422D, D574E, W575F, R308K, R275H, **D490K**[1]

1The bold mutations were chosen for further work.

„No mutation success” means here that there is no visible change observed in the iGENE VISION. Functionally this means that these mutants are the most different ones when compared to the WT enzyme. The K312V, Y267W, A349P and D490K from four different levels were chosen for further work. The aim was to have a closer look to four levels of the „metasystem PerZan”.

5.3 Characterization of the four DNA polymerase λ mutants after purification

After the three main steps of purification (PC, HisTrap, HiTrap) the pol λ mutants A349P, K312V, Y267W and D490K were characterized by SDS-PAGE, by western blot analysis and for nuclease contamination. Figure 2A shows that the four enzymes were all over 90% pure. The western blot analysis showed that all enzymes are indeed pol λ (Figure 2B) and finally the nuclease assay showed the absence of contaminating nucleases in the amount range (25-200 ng) used in this work (Figure 2C).

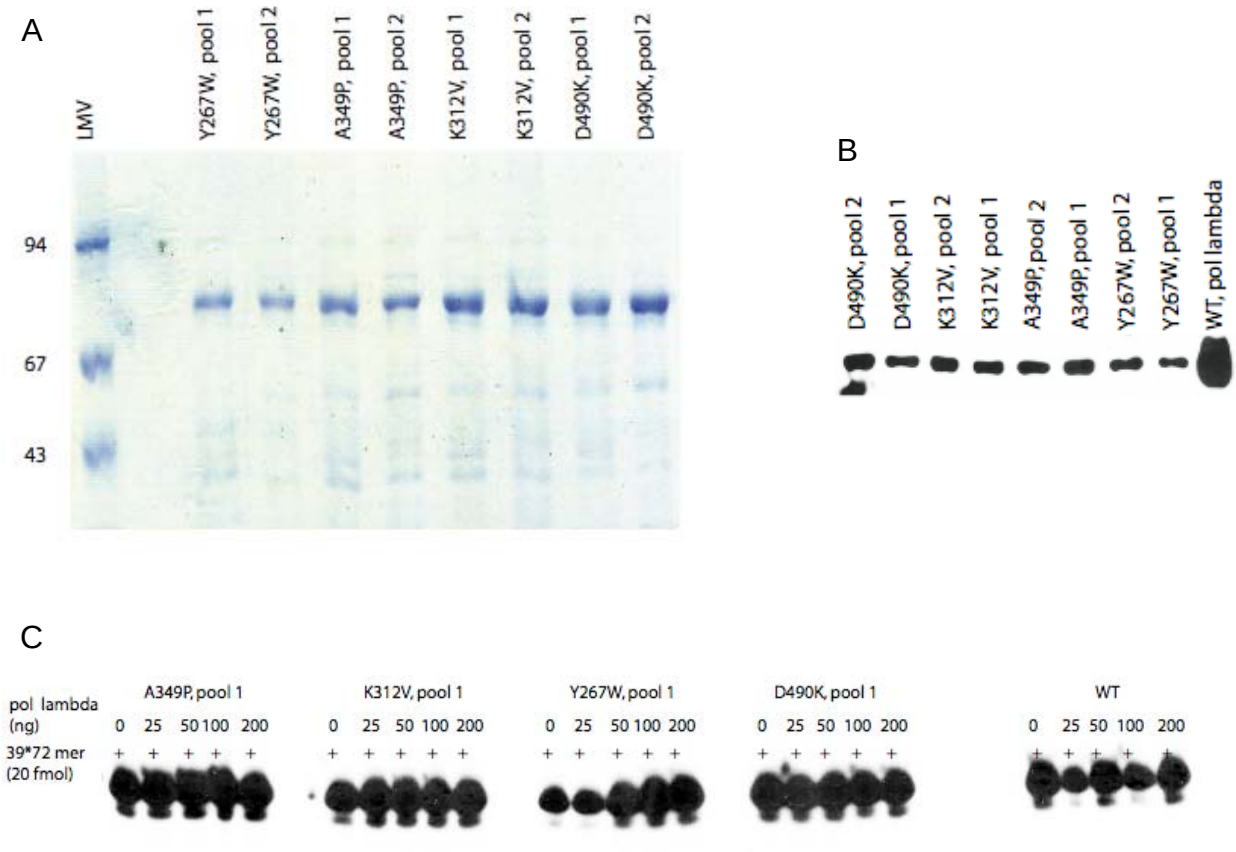

Figure 2: Characterization of the four DNA polymerase λ mutants. The experiments were performed as outlined in Materials and Methods. **A)** SDS-PAGE and coomassie staining, **B)** Western blot analysis, **C)** Nuclease assay.

5.4 *Titration of the four DNA polymerase λ mutants on a 39/72 mer primer/template*

First the four pol λ mutants and the WT were titrated over a control undamaged 39/72 mer primer/template. The results showed that K312V had a similar DNA synthesis pattern as the WT, while the Y267W and the A349P showed reduced incorporation. The D490K was catalytically inactive (Figure 3A). The quantified products are documented in Figure 3B. With 50 ng of the enzyme the pol λ mutant K312V lead to 96% of activity in comparison to the WT, Y267W showed 71%, A349P 24% and D490K had less than 0.1% (Figure 3C).

A

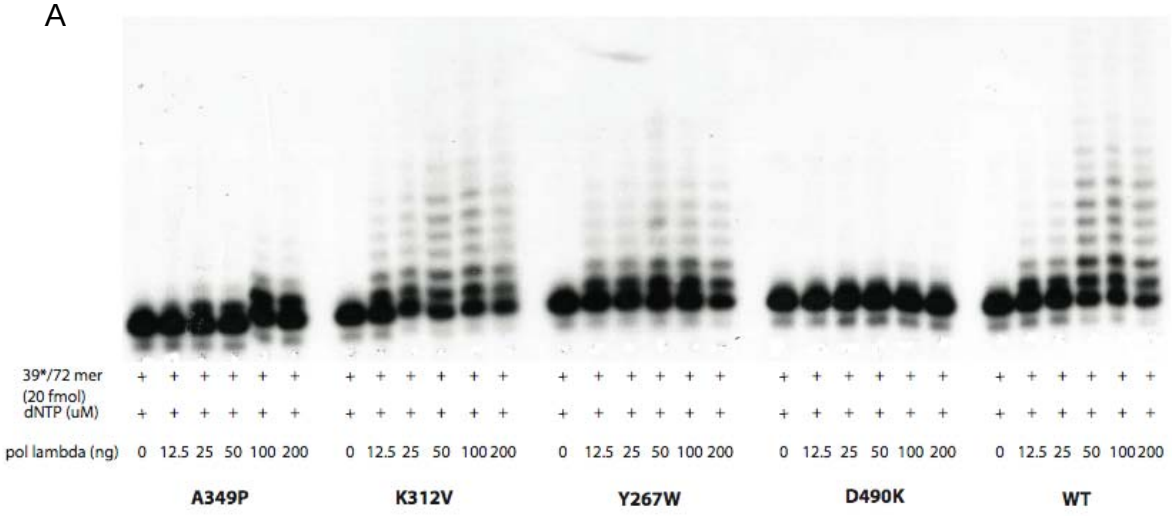

B

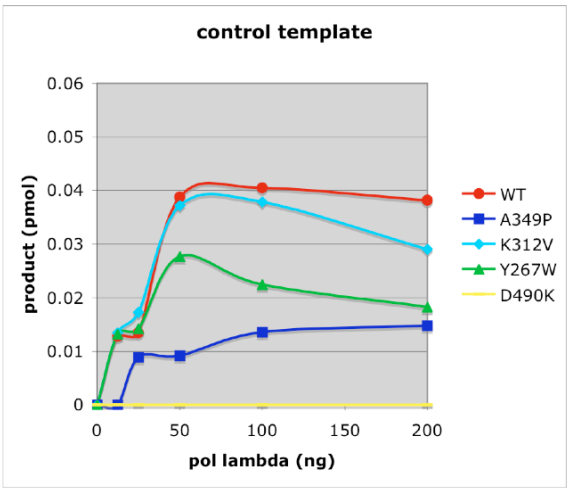

C

Pol λ	%
WT	100
K312V	96
Y267W	71
A349P	24
D490K	< 0.1

Figure 3: Titration of the four DNA polymerase λ mutants on a 39/72 mer primer/template. The experiments were performed as outlined in Materials and

Methods. **A**) Increasing amounts of pol λ were titrated with a constant amount of dNTPs and control primer/template and quantified with Adobe Photoshop CS3 as seen in **B**). Summarized in **C**) is the resulting order of their activities.

5.5 Titration of the four DNA polymerase λ mutants on a 39/8oxoG72 mer primer/template

Next it was of interest to test how the pol λ mutants behave over a 39/8oxoG72 mer primer/template. It was the same primer/template as used in Figure 3 but with an 8-oxo-G lesion immediately after the primer.

It is known that pol λ is a protection shield against exactly these oxidative damages, since it can incorporate the correct C opposite an 8-oxo-G and thus corrects the mistakes made by the replication machinery, which often incorporates the wrong A opposite an 8-oxo-G. Pol λ allows the correct incorporation of dCTP opposite an 8-oxo-G template 12-fold more efficiently than the incorrect dATP (Maga et al., 2007). Therefore it was of interest to test the four pol λ mutants on this 8-oxo-G lesion.

The data in Figure 4 showed that the pol λ mutants K312V and Y267W produced more incorporation products than A349P and that D490K was again inactive. The data were again quantified as in Figure 3 and showed that the hierarchy with the 8-oxo-G template corresponds to the control template (compare Figure 3C and 4C).

A

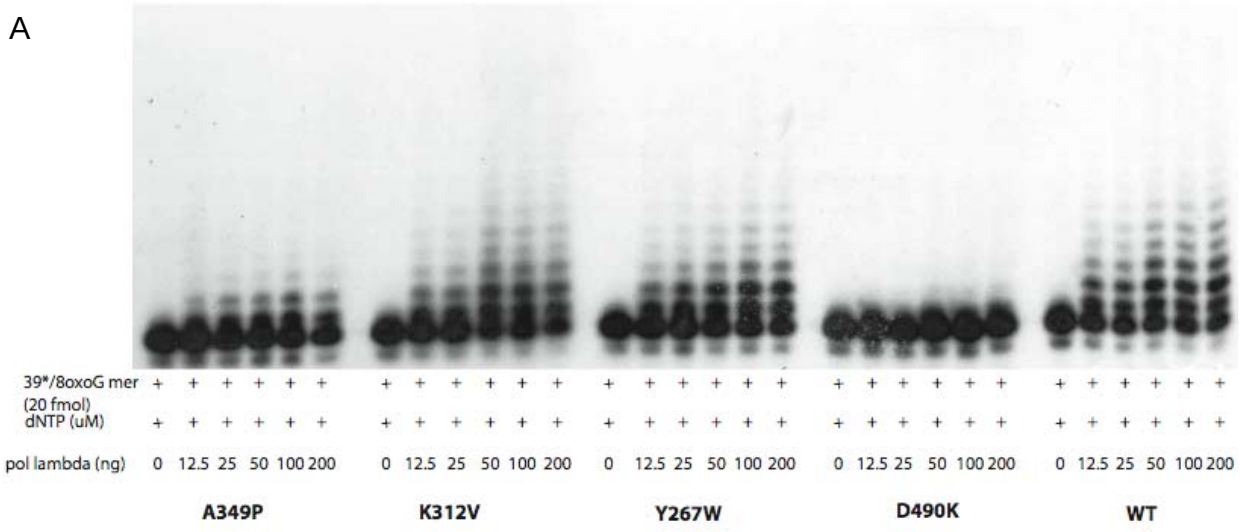

B

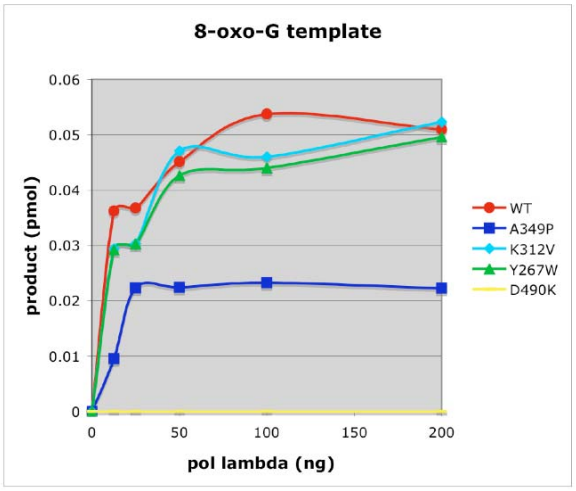

C

Pol λ	%
WT	100
K312V	83
Y267W	82
A349P	61
D490K	< 0.1

Figure 4: Titration of the four DNA polymerase λ mutants on a 39/8oxoG 72 mer primer/template. The experiments were performed as outlined in Materials and Methods. **A**) An increasing amount of pol λ was titrated with a constant amount of dNTPs and 8-oxo-G primer/template and quantified with Adobe Photoshop CS3 as seen in **B**). Summarized in **C**) is the resulting order of their activities.

5.6 Titration of the four DNA polymerase λ mutants on 39/72 mer and on 39/8oxoG72 mer primer/templates

The next set of experiments was performed side by side by testing the enzyme on a control and on an 8-oxo-G template. Again, the samples were prepared as described before, but to make sure that a comparison is possible, the same master mix was used for both primer/templates tested. The master mix was divided in two and in one part the control template and in the other part the template with the 8-oxo-G lesion was added. Then the reaction was started by adding 9 µl of this reaction mix to pol λ dilutions and the further procedure was like before.

The data suggested (Figure 5A) that in each case synthesis over 8-oxo-G was reduced (Figure 5B). When the results were quantified, the WT pol λ showed 78% of activity over the 8-oxo-G template when compared to the control template. The mutants showed 65% for K312V, 62% for Y267W and 53% for A349P. Again the D490K was inactive. In summary the same hierarchy was evident as already observed in Figure 3 and 4 being WT > K312V > Y267W > A349P >>> D490K.

A

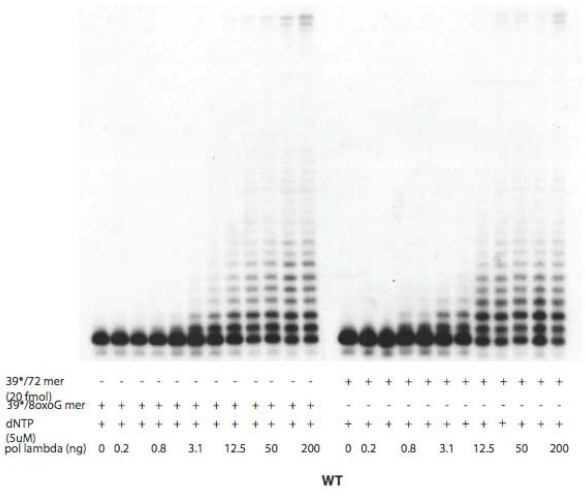
39*/72 mer (20 fmol)
39*/8oxoG mer
dNTP (5uM)
pol lambda (ng)
0 0.2 0.8 3.1 12.5 50 200 0 0.2 0.8 3.1 12.5 50 200
WT

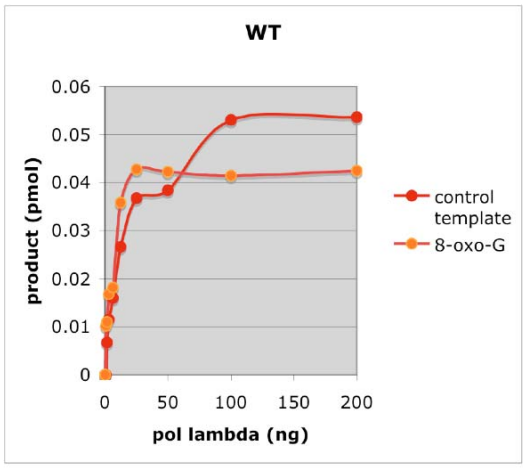
WT
product (pmol)
0.06
0.05
0.04
0.03
0.02
0.01
0
0 50 100 150 200
pol lambda (ng)
control template
8-oxo-G

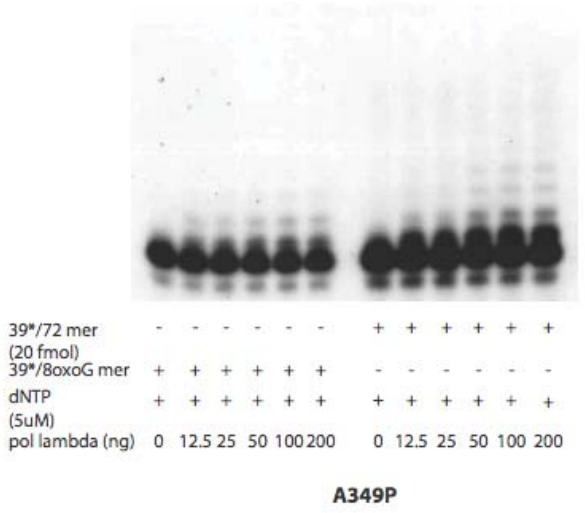
39*/72 mer (20 fmol)
39*/8oxoG mer
dNTP (5uM)
pol lambda (ng)
0 12.5 25 50 100 200 0 12.5 25 50 100 200
A349P

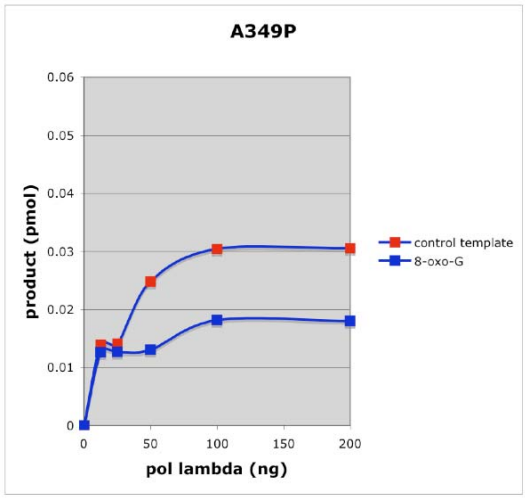
A349P
product (pmol)
0.06
0.05
0.04
0.03
0.02
0.01
0
0 50 100 150 200
pol lambda (ng)
control template
8-oxo-G

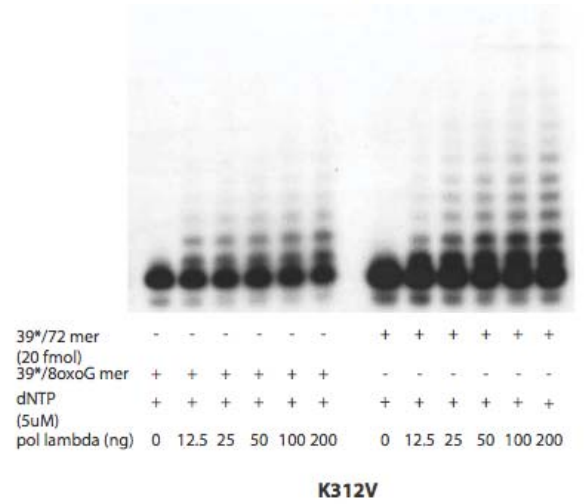
39*/72 mer (20 fmol)
39*/8oxoG mer
dNTP (5uM)
pol lambda (ng)
0 12.5 25 50 100 200 0 12.5 25 50 100 200
K312V

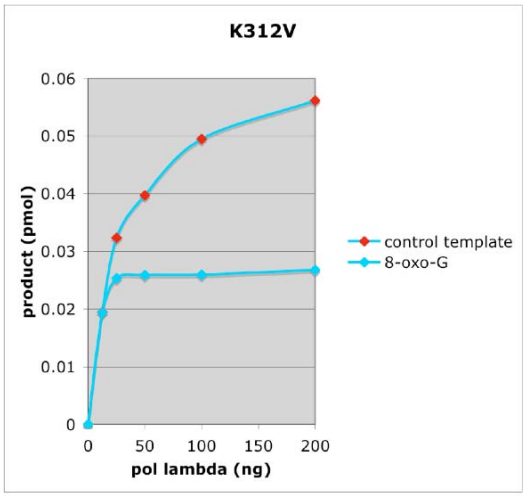
K312V
product (pmol)
0.06
0.05
0.04
0.03
0.02
0.01
0
0 50 100 150 200
pol lambda (ng)
control template
8-oxo-G

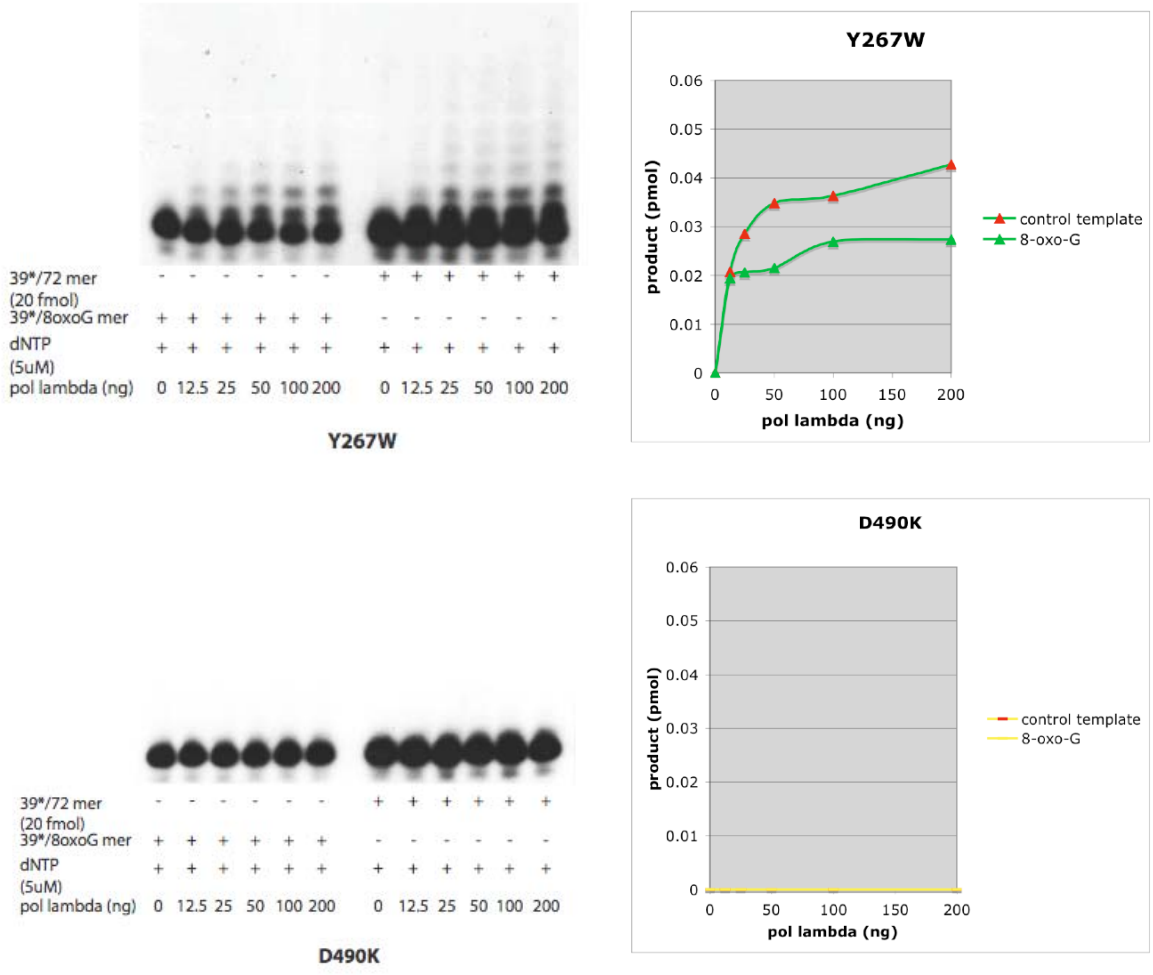

B

Pol λ		WT	K312V	Y267W	A349P	D490K
control template	%	100	100	100	100	< 0.1
8-oxo-G template		78	65	62	53	< 0.1

Figure 5: Titration of the four DNA polymerase λ mutants on 39/72 mer and on 39/8oxoG72mer primer/templates. The experiments were performed as outlined in Materials and Methods. **A**) An increasing amount of pol λ enzyme was titrated with a constant amount of dNTPs, control and 8-oxo-G primer/template and quantified with Adobe Photoshop CS3. Summarized in **B**) is the order of activities shown.

5.7 Titration of dNTP's in the presence of a constant amount of the four DNA polymerase λ mutants on 39/72 mer and on 39/8oxoG72 mer primer/templates

So far, the amount of dNTPs was kept constant and the pol λ mutants and the WT were titrated. With these experiments the same order in the activity was always showed, namely that K312V is more active than Y267W. These two have apparently more activity than A349P and with D490K no activity could be seen (compare Figures 3C, 4C and 5B). In the following experiment dNTPs were titrated and the amount of enzyme was kept constant.

1) V_{max} is the maximal rate at which an enzyme catalyzes a reaction. It is expressed as the amount of product formed per minute. So the V_{max} shows how fast pol λ incorporates its substrat (dNTPs). A low V_{max} means that the enzyme incorporates its substrate slowly.

2) K_m represents the substrate concentration at half of V_{max} of the enzyme. It is a measurement of the apparent affinity of the enzyme for the substrate. In other words, it indicates how well the substrate is binding the enzyme. Therefore with a low K_m the affinity for the substrate is high.

3) K_{cat} is a measurement of the turnover of the enzyme. It says which amount of dNTP is incorporated per minute.

4) K_{cat}/K_m describes the relative specificity of a fixed amount of the enzyme for its substrate being the parameter showing the enzyme efficiency.

Since the main interest was to analyse the pol λ efficiency, the K_{cat}/K_m were finally compared. The mutant K312V showed a higher K_{cat}/K_m value than the WT (Figure 6B) while Y267W was about equal. The K_{cat}/K_m value of the A349P was 10 times reduced compared to the WT. The D490K was again inactive. In summary with these experiments a different hierarchy was observed, being K312V > Y267W > WT >> A349P >>> D490K.

A

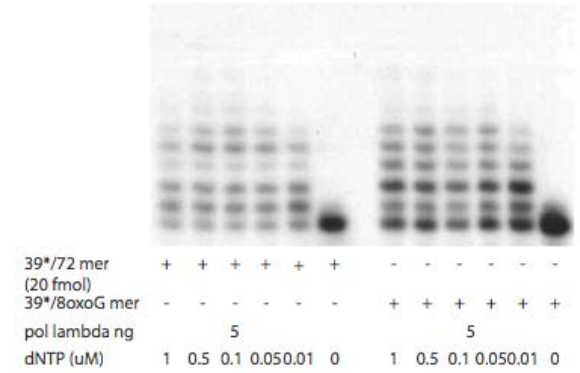

WT

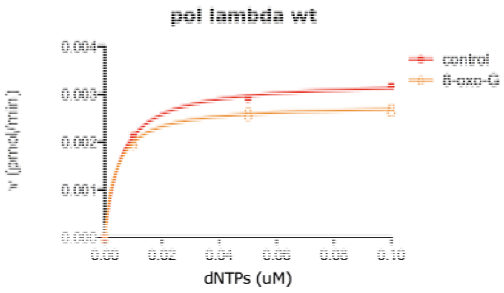

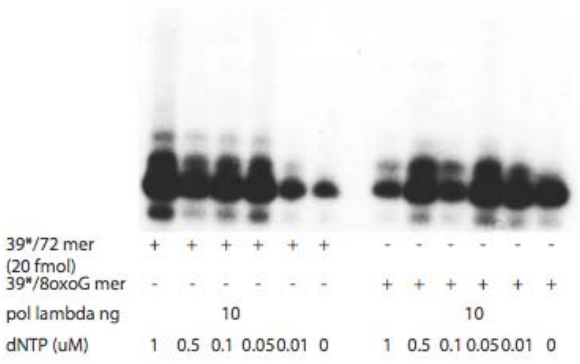

A349P

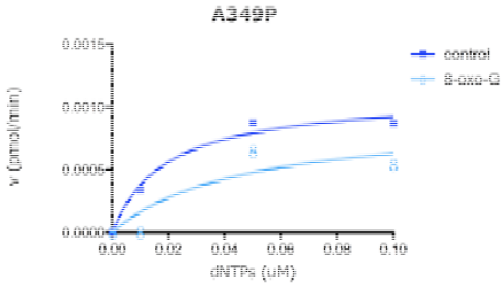

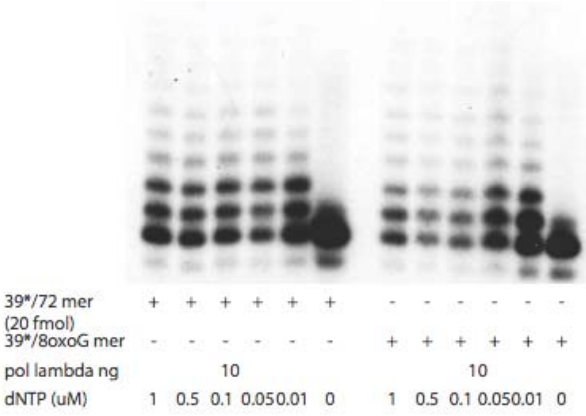

K312V

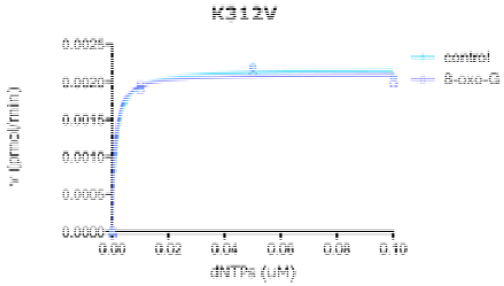

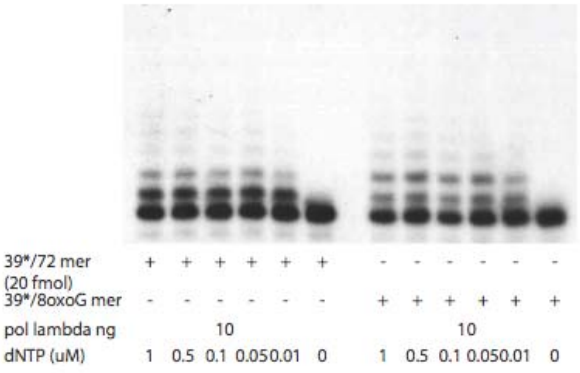

Y267W

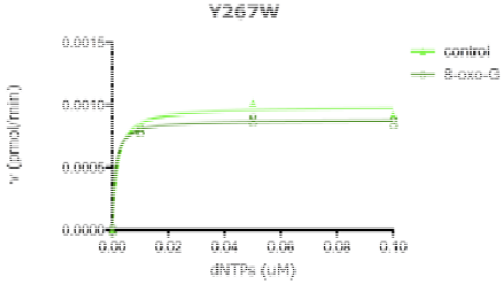

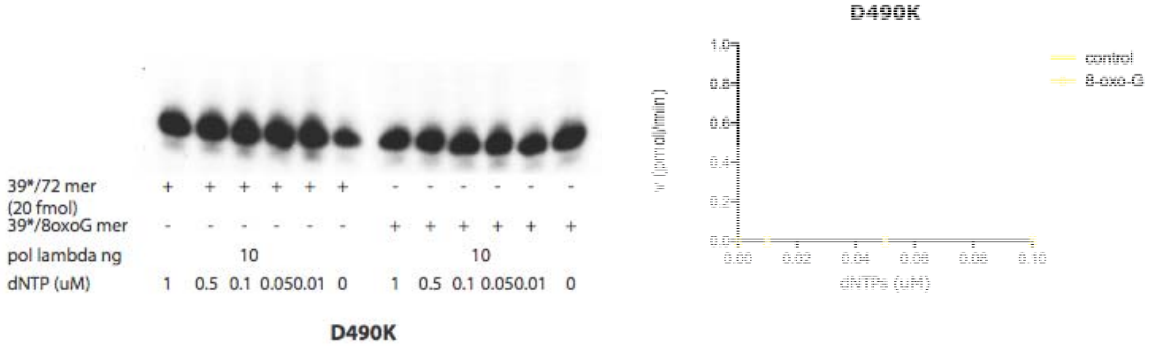

B

Pol λ	template	K_m (μM)	K_{cat} (min^{-1})	V_{max} ($\mu M min^{-1}$)	K_{cat}/K_m ($min^{-1}\mu M^{-1}$)
WT	control	$5.6x10^{-3}$	0.41	$3.3x10^{-3}$	73.25
	8-oxo-G	$4.0x10^{-3}$	0.35	$2.8x10^{-3}$	87.39
K312V	control	$1.3x10^{-3}$	0.27	$2.2x10^{-3}$	210.61
	8-oxo-G	$0.9x10^{-3}$	0.26	$2.1x10^{-3}$	301.35
Y267W	control	$1.6x10^{-3}$	0.12	$1.0x10^{-3}$	73.13
	8-oxo-G	$1.0x10^{-3}$	0.11	$0.9x10^{-3}$	111.94
A349P	control	$19.1x10^{-3}$	0.14	$1.1x10^{-3}$	7.33
	8-oxo-G	$46x10^{-3}$	0.11	$1.0x10^{-3}$	2.39
D490K	control	not applicable	not applicable	not applicable	not applicable
	8-oxo-G	not applicable	not applicable	not applicable	not applicable

Figure 6: Titration of dNTP`s in the presence of a constant amount of the four DNA polymerase λ mutants on 39/72 mer and on 39/8oxoG72 mer primer/templates. The experiments were performed as outlined in Materials and Methods. **A**) Different amounts of dNTPs were titrated with a constant amount of pol λ on a control and an 8-oxo-G primer/template and quantified with Adobe Photoshop CS3. Summarized in **B**) are K_m, K_{cat}, V_{max} and K_{cat}/K_m.

5.8 Single nucleotide dCTP and dATP titrations of the four DNA polymerase λ mutants on 39/72 mer and on 39/8oxoG72 mer primer/templates

The experiments so far always contained the four dNTPs. In the final experiment only dCTPs and dATPs were tested individually. For each reaction 6 different dCTP and dATP concentrations were tested with a constant amount of pol λ. When the bias of correct C versus incorrect A incorporation was tested a novel hierarchy appeared, being A349P > WT > Y267W> K312V >>>D490K, which is the exact opposite observed so far (with the exception of the inactive mutant D490K). In this experiment, in which only a single dNTP was tested, the hierarchy changed in contrast to the synthesis tested with the complete set of four nucleotides.

A

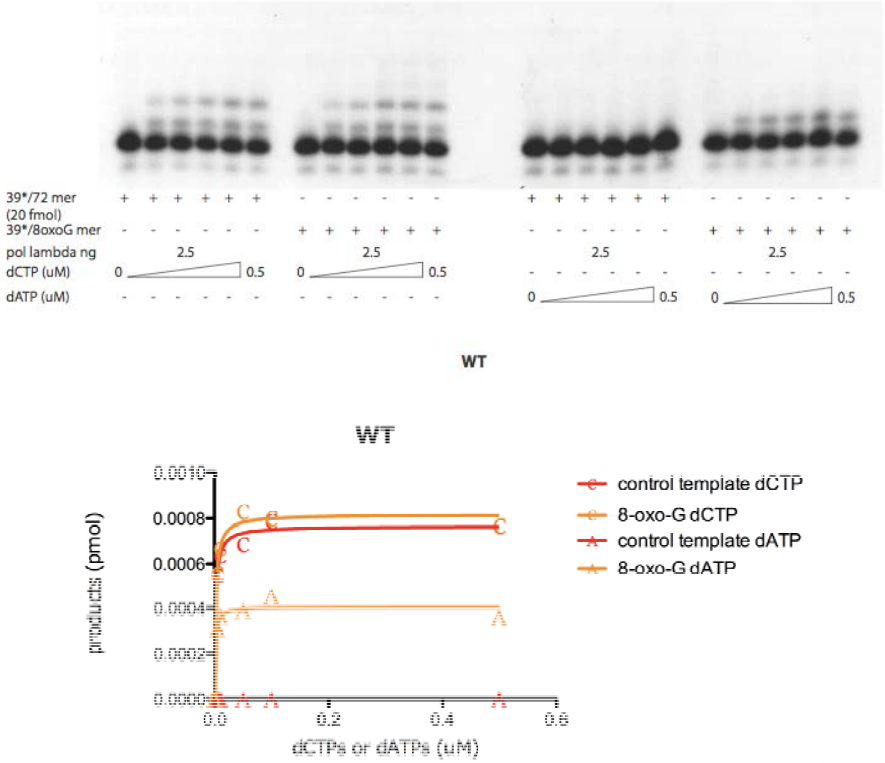

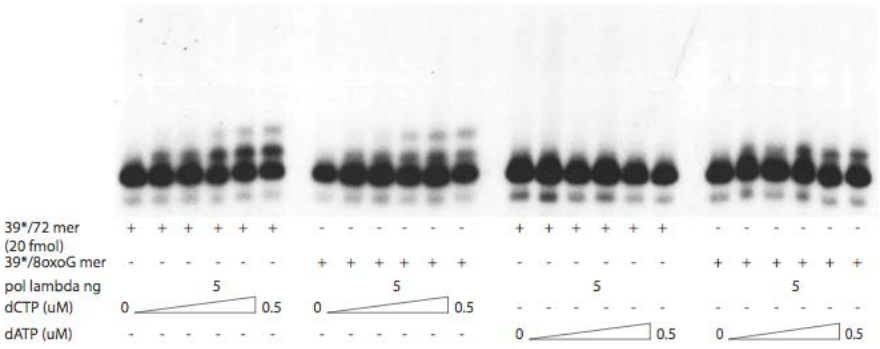
39*/72 mer
(20 fmol)
39*/8oxoG mer
pol lambda ng
dCTP (uM)
dATP (uM)
5
0
0.5

A349P

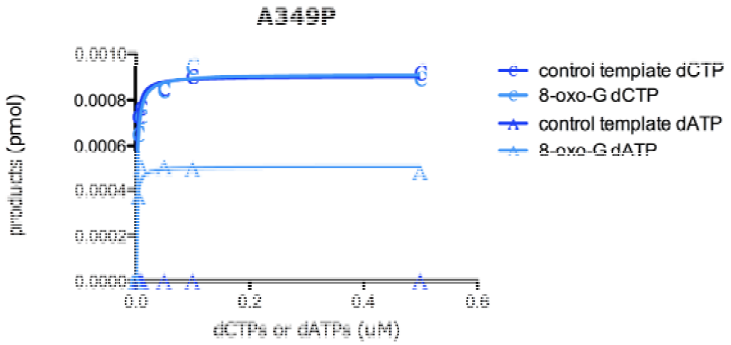
A349P
products (pmol)
0.0010
0.0008
0.0006
0.0004
0.0002
0.0000
0.0
0.2
0.4
0.6
dCTPs or dATPs (uM)
control template dCTP
8-oxo-G dCTP
control template dATP
8-oxo-G dATP

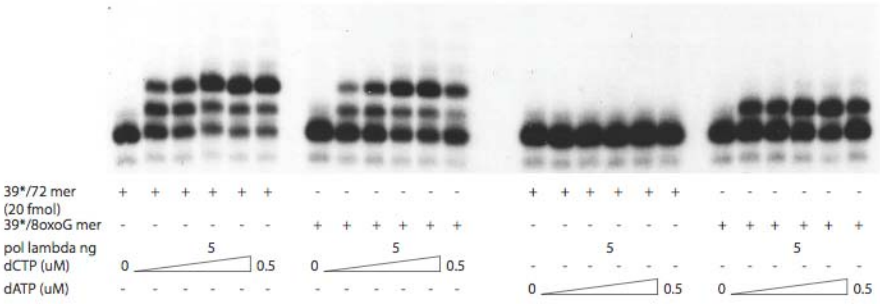
39*/72 mer
(20 fmol)
39*/8oxoG mer
pol lambda ng
dCTP (uM)
dATP (uM)
5
0
0.5

K312V

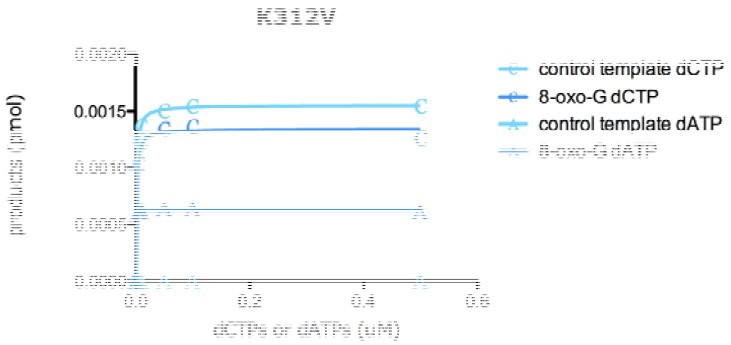
K312V
0.0015
0.0010
0.0005
0.0000
0.0
0.2
0.4
0.6
dCTPs or dATPs (uM)
8-oxo-G dCTP
control template dATP

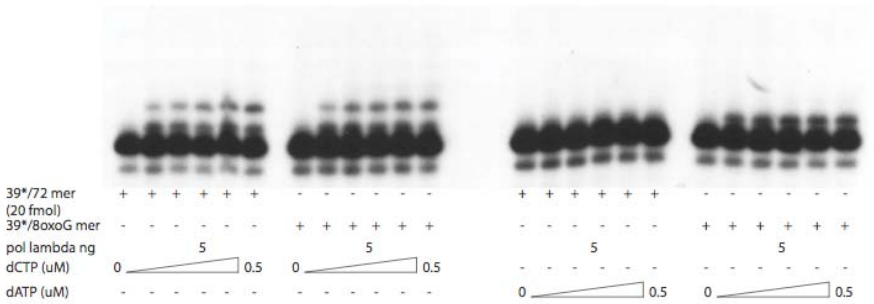
39*/72 mer (20 fmol)
39*/8oxoG mer
pol lambda ng
dCTP (uM)
dATP (uM)
5
0
0.5

Y267W

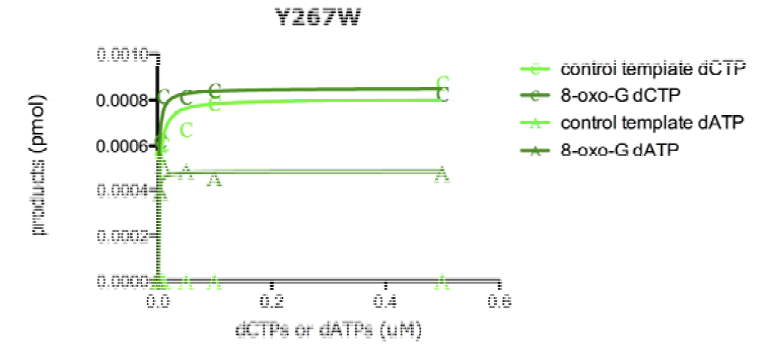
Y267W
products (pmol)
dCTPs or dATPs (uM)
control template dCTP
8-oxo-G dCTP
control template dATP
8-oxo-G dATP

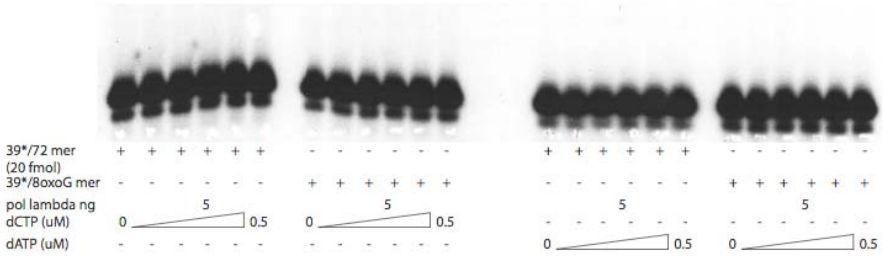
39*/72 mer (20 fmol)
39*/8oxoG mer
pol lambda ng
dCTP (uM)
dATP (uM)
5
0
0.5

D490K

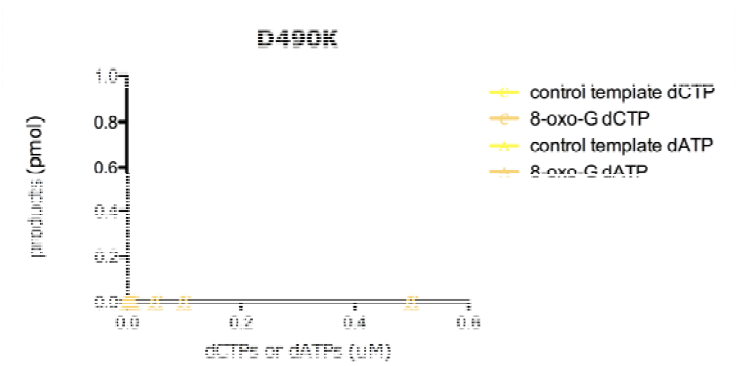
D490K
products (pmol)
dCTPs or dATPs (uM)
control template dCTP
8-oxo-G dCTP
control template dATP
8-oxo-G dATP

B

Pol λ	dNTPs	template	K_m (μM)	K_{cat} (min-1)	V_{max} (μMmin-1)	K_{cat}/K_m (min-1μM-1)	C:A
WT	dCTP	control	2.1x10-3	0.1	0.8x10-3	48.57	2.60
		8-oxo-G	2.2x10-3	0.1	0.8x10-3	45.33	
	dATP	control	not applicable				
		8-oxo-G	1.4x10-3	0.05	0.9x10-3	78.91	
K312V	dCTP	control	1.3x10-3	0.19	1.6x10-3	146.04	0.33
		8-oxo-G	1.3x10-3	0.17	1.4x10-3	129.67	
	dATP	control	not applicable				
		8-oxo-G	0.1x10-3	0.08	0.6x10-3	618.71	
Y267W	dCTP	control	2.7x10-3	0.1	0.8x10-3	37.13	1.25
		8-oxo-G	1.4x10-3	0.1	0.9x10-3	72.05	
	dATP	control	not applicable				
		8-oxo-G	0.7x10-3	0.06	0.48x10-3	87.68	
A349P	dCTP	control	1.4x10-3	0.11	0.9x10-3	78.91	3.13
		8-oxo-G	2.2x10-3	0.11	0.9x10-3	50.21	
	dATP	control	not applicable				
		8-oxo-G	1.3x10-3	0.06	0.5x10-3	42.21	
D490K	dCTP	control	not applicable	not applicable	not applicable	not applicable	
		8-oxo-G	not applicable	not applicable	not applicable	not applicable	
	dATP	control	not applicable				
		8-oxo-G	not applicable	not applicable	not applicable	not applicable	

Figure 7: Single nucleotide dCTP and dATP titrations of the four DNA polymerase λ mutants on 39/72 mer and on 39/8oxoG72 mer primer/templates. The experiments were performed as outlined in Materials and Methods. **A**) Increasing amounts of dCTP and dATP were titrated with a constant amount of pol λ on control and on 8-oxo-G primer/templates and quantified with Adobe Photoshop CS3. The values were summarized in **B**). The ration of C to A (last column) shows again the hierarchy: A349P > WT > Y267W >> K312V >>> D490K.

6 Discussion

The aim of this thesis was to scientifically verify predictions made by the „metasystem PerZan". 20 pol λ mutants, generated *in silico,* were analyzed by Karsten Knut Panzer with his „metasystem PerZan". According to this, the mutants were subdivided into 5 classes of mutational success, whereof four different mutants have been chosen, being A349P, K312V, Y267W and D490K. The pol λ mutant protein were generated by site-directed mutagenesis, transformed and expressed in *E. coli* and finally purified. These four pol λ mutants were subjected to scientific verification. In the starting experiments pol λ WT and mutants were titrated and analyzed over 39/72 mer and 39/8oxoG72 mer primer/templates. Firstly, on a control primer/template it was found that the pol λ mutant K312V achieved 96% of activity in comparison to the WT, Y267W 71%, A349P 24%. The D490K mutant was as expected inactive (< 0.1%). Secondly, the pol λ mutants were titrated over a template containing an 8-oxo-G lesion. It was found that K312V arrived 83% of activity in comparison to the WT, Y267W 82% and A349P 61%. D490K again was inactive. Thirdly, each of the four mutants and the WT pol λ were titrated over a control and an 8-oxo-G primer/template in the same gel. Furthermore dNTP's were titrated in similar experiments. These experiments suggested a similar hierarchy, namely that K312V was more active and efficient than Y267W and these two more than A349P. The mutant D490K was inactive in all experiments. This was the same order as the „metasystem PerZan" has predicted.

Furthermore it is known that pol λ can incorporate a correct dCTP opposite an 8-oxo-G site 12 times more efficiently than the wrong dATP (Maga et al., 2007). According to this observation the mutants were tested in their activity to incorporate the single nucleotides dCTP and dATP. By analyzing the K_{cat}/K_m, we found that the A349P mutant was more efficient than Y267W. Both were more efficient than K312V and with D490K again no incorporation was observed. The so far weak mutant A349P was incorporating a correct dCTP better opposite 8-oxo-G than all the other mutants and also the WT. In

this single nucleotide incorporation experiments another hierarchy was observed, not corresponding to the predictions of the „metasystem PerZan”.

From these studies it was conclude that the „metasystem PerZan” was right in predicting the mutation order as long as the experiments were done with all four nucleotides. The „metasystem PerZan” was however overstrained when asked for specific parameters such as V_{max}, K_m, K_{cat} and K_{cat}/K_m. To proof the principle further, one could chose four different mutants from the same level of „mutation success” predicted by the „metasystem PerZan”. It would then be interesting to see if such mutants have the same activity and efficiency.

In conclusion, the „metasystem PerZan” is more than just a fantasy and might give an overview, but the current data cannot yet admit that the proof of principle has been achieved for the „metasystem PerZan”. For this experiments with more mutants and other test systems would be required. They could e.g. include for K312V dRPlyase assays, for Y267W gap filling assays and for A349P DNA binding assays.

7 References

Beard, W.A., Shock, D.D., Vande Berg, B.J., and Wilson, S.H. (2002). Efficiency of correct nucleotide insertion governs DNA polymerase fidelity. J Biol Chem *277*, 47393-47398.

Braithwaite, E.K., Kedar, P.S., Lan, L., Polosina, Y.Y., Asagoshi, K., Poltoratsky, V.P., Horton, J.K., Miller, H., Teebor, G.W., Yasui, A.*, et al.* (2005a). DNA polymerase lambda protects mouse fibroblasts against oxidative DNA damage and is recruited to sites of DNA damage/repair. J Biol Chem *280*, 31641-31647.

Braithwaite, E.K., Prasad, R., Shock, D.D., Hou, E.W., Beard, W.A., and Wilson, S.H. (2005b). DNA polymerase lambda mediates a back-up base excision repair activity in extracts of mouse embryonic fibroblasts. J Biol Chem *280*, 18469-18475.

Burrows, C.J., and Muller, J.G. (1998). Oxidative Nucleobase Modifications Leading to Strand Scission. Chem Rev *98*, 1109-1152.

Christmann, M., Tomicic, M.T., Roos, W.P., and Kaina, B. (2003). Mechanisms of human DNA repair: an update. Toxicology *193*, 3-34.

David, S.S., O'Shea, V.L., and Kundu, S. (2007). Base-excision repair of oxidative DNA damage. Nature *447*, 941-950.

Delarue, M., Boule, J.B., Lescar, J., Expert-Bezancon, N., Jourdan, N., Sukumar, N., Rougeon, F., and Papanicolaou, C. (2002). Crystal structures of a template-independent DNA polymerase: murine terminal deoxynucleotidyltransferase. EMBO J *21*, 427-439.

Fan, W., and Wu, X. (2004). DNA polymerase lambda can elongate on DNA substrates mimicking non-homologous end joining and interact with XRCC4-ligase IV complex. Biochem Biophys Res Commun *323*, 1328-1333.

Featherstone, C., and Jackson, S.P. (1999). Ku, a DNA repair protein with multiple cellular functions? Mutat Res *434*, 3-15.

Foiani, M., Pellicioli, A., Lopes, M., Lucca, C., Ferrari, M., Liberi, G., Muzi Falconi, M., and Plevani, P. (2000). DNA damage checkpoints and DNA replication controls in Saccharomyces cerevisiae. Mutat Res *451*, 187-196.

Friedberg, E.C., Walker, G.C., and Siede, W. (1995). DNA repair and mutagenesis (Washington, D.C., ASM Press).

Frosina, G., Fortini, P., Rossi, O., Carrozzino, F., Raspaglio, G., Cox, L.S., Lane, D.P., Abbondandolo, A., and Dogliotti, E. (1996). Two pathways for base excision repair in mammalian cells. J Biol Chem *271*, 9573-9578.

Garcia-Diaz, M., Bebenek, K., Gao, G., Pedersen, L.C., London, R.E., and Kunkel, T.A. (2005). Structure-function studies of DNA polymerase lambda. DNA Repair (Amst) *4*, 1358-1367.

Garcia-Diaz, M., Bebenek, K., Krahn, J.M., Blanco, L., Kunkel, T.A., and Pedersen, L.C. (2004). A structural solution for the DNA polymerase lambda-dependent repair of DNA gaps with minimal homology. Mol Cell *13*, 561-572.

Garcia-Diaz, M., Bebenek, K., Kunkel, T.A., and Blanco, L. (2001). Identification of an intrinsic 5'-deoxyribose-5-phosphate lyase activity in human DNA polymerase lambda: a possible role in base excision repair. J Biol Chem *276*, 34659-34663.

Garcia-Diaz, M., Bebenek, K., Sabariegos, R., Dominguez, O., Rodriguez, J., Kirchhoff, T., Garcia-Palomero, E., Picher, A.J., Juarez, R., Ruiz, J.F.*, et al.* (2002). DNA polymerase lambda, a novel DNA repair enzyme in human cells. J Biol Chem *277*, 13184-13191.

Garcia-Diaz, M., Dominguez, O., Lopez-Fernandez, L.A., de Lera, L.T., Saniger, M.L., Ruiz, J.F., Parraga, M., Garcia-Ortiz, M.J., Kirchhoff, T., del Mazo, J.*, et al.* (2000). DNA polymerase lambda (Pol lambda), a novel eukaryotic DNA polymerase with a potential role in meiosis. J Mol Biol *301*, 851-867.

Haber, J.E. (1998). The many interfaces of Mre11. Cell *95*, 583-586.

Hoeijmakers, J.H. (2001). Genome maintenance mechanisms for preventing cancer. Nature *411*, 366-374.

Hubscher, U., Maga, G., and Spadari, S. (2002). Eukaryotic DNA polymerases. Annu Rev Biochem *71*, 133-163.

Jackson, S.P. (2002). Sensing and repairing DNA double-strand breaks. Carcinogenesis *23*, 687-696.

Kelman, Z., and O'Donnell, M. (1994). DNA replication: enzymology and mechanisms. Curr Opin Genet Dev *4*, 185-195.

Klaunig, J.E., and Kamendulis, L.M. (2004). The role of oxidative stress in carcinogenesis. Annu Rev Pharmacol Toxicol *44*, 239-267.

Lee, J.W., Blanco, L., Zhou, T., Garcia-Diaz, M., Bebenek, K., Kunkel, T.A., Wang, Z., and Povirk, L.F. (2004). Implication of DNA polymerase lambda in alignment-based gap filling for nonhomologous DNA end joining in human nuclear extracts. J Biol Chem *279*, 805-811.

Lindahl, T. (1993). Instability and decay of the primary structure of DNA. Nature *362*, 709-715.

Lodish, H.F., and Darnell, J.E. (1995). Molecular cell biology, 3rd edn (New York, Scientific American Books : Distributed by W.H. Freeman and Co.).

Ma, Y., Lu, H., Schwarz, K., and Lieber, M.R. (2005). Repair of double-strand DNA breaks by the human nonhomologous DNA end joining pathway: the iterative processing model. Cell Cycle *4*, 1193-1200.

Ma, Y., Lu, H., Tippin, B., Goodman, M.F., Shimazaki, N., Koiwai, O., Hsieh, C.L., Schwarz, K., and Lieber, M.R. (2004). A biochemically defined system for mammalian nonhomologous DNA end joining. Mol Cell *16*, 701-713.

Maciejewski, M.W., Shin, R., Pan, B., Marintchev, A., Denninger, A., Mullen, M.A., Chen, K., Gryk, M.R., and Mullen, G.P. (2001). Solution structure of a viral DNA repair polymerase. Nat Struct Biol *8*, 936-941.

Maga, G., Crespan, E., Wimmer, U., van Loon, B., Amoroso, A., Mondello, C., Belgiovine, C., Ferrari, E., Locatelli, G., Villani, G.*, et al.* (2008). Replication protein A and proliferating cell nuclear antigen coordinate DNA polymerase selection in 8-oxo-guanine repair. Proc Natl Acad Sci U S A *105*, 20689-20694.

Maga, G., Villani, G., Crespan, E., Wimmer, U., Ferrari, E., Bertocci, B., and Hubscher, U. (2007). 8-oxo-guanine bypass by human DNA polymerases in the presence of auxiliary proteins. Nature *447*, 606-608.

Maga, G., Villani, G., Ramadan, K., Shevelev, I., Tanguy Le Gac, N., Blanco, L., Blanca, G., Spadari, S., and Hubscher, U. (2002). Human DNA polymerase lambda functionally and physically interacts with proliferating cell nuclear antigen in normal and translesion DNA synthesis. J Biol Chem *277*, 48434-48440.

Matsumoto, Y., and Kim, K. (1995). Excision of deoxyribose phosphate residues by DNA polymerase beta during DNA repair. Science *269*, 699-702.

Matsumoto, Y., Kim, K., and Bogenhagen, D.F. (1994). Proliferating cell nuclear antigen-dependent abasic site repair in Xenopus laevis oocytes: an alternative pathway of base excision DNA repair. Mol Cell Biol *14*, 6187-6197.

Maya, R., Balass, M., Kim, S.T., Shkedy, D., Leal, J.F., Shifman, O., Moas, M., Buschmann, T., Ronai, Z., Shiloh, Y.*, et al.* (2001). ATM-dependent phosphorylation of Mdm2 on serine 395: role in p53 activation by DNA damage. Genes Dev *15*, 1067-1077.

Memisoglu, A., and Samson, L. (2000). Base excision repair in yeast and mammals. Mutat Res *451*, 39-51.

Moshous, D., Callebaut, I., de Chasseval, R., Corneo, B., Cavazzana-Calvo, M., Le Deist, F., Tezcan, I., Sanal, O., Bertrand, Y., Philippe, N.*, et al.* (2001). Artemis, a novel DNA double-strand break repair/V(D)J recombination protein, is mutated in human severe combined immune deficiency. Cell *105*, 177-186.

Neeley, W.L., and Essigmann, J.M. (2006). Mechanisms of formation, genotoxicity, and mutation of guanine oxidation products. Chem Res Toxicol *19*, 491-505.

Nick McElhinny, S.A., and Ramsden, D.A. (2004). Sibling rivalry: competition between Pol X family members in V(D)J recombination and general double strand break repair. Immunol Rev *200*, 156-164.

Petrini, J.H. (2000). The Mre11 complex and ATM: collaborating to navigate S phase. Curr Opin Cell Biol *12*, 293-296.

Ramadan, K., Shevelev, I., and Hubscher, U. (2004). The DNA-polymerase-X family: controllers of DNA quality? Nat Rev Mol Cell Biol *5*, 1038-1043.

Rooney, S., Chaudhuri, J., and Alt, F.W. (2004). The role of the non-homologous end-joining pathway in lymphocyte development. Immunol Rev *200*, 115-131.

Showalter, A.K., Byeon, I.J., Su, M.I., and Tsai, M.D. (2001). Solution structure of a viral DNA polymerase X and evidence for a mutagenic function. Nat Struct Biol *8*, 942-946.

Sobol, R.W., and Wilson, S.H. (2001). Mammalian DNA beta-polymerase in base excision repair of alkylation damage. Prog Nucleic Acid Res Mol Biol *68*, 57-74.

Steitz, T.A. (1999). DNA polymerases: structural diversity and common mechanisms. J Biol Chem *274*, 17395-17398.

Takata, M., Sasaki, M.S., Sonoda, E., Morrison, C., Hashimoto, M., Utsumi, H., Yamaguchi-Iwai, Y., Shinohara, A., and Takeda, S. (1998). Homologous recombination and non-homologous end-joining pathways of DNA double-strand break repair have overlapping roles in the maintenance of chromosomal integrity in vertebrate cells. EMBO J *17*, 5497-5508.

Wimmer, U., Ferrari, E., Hunziker, P., and Hubscher, U. (2008). Control of DNA polymerase lambda stability by phosphorylation and ubiquitination during the cell cycle. EMBO Rep *9*, 1027-1033.

Wu, X., Wilson, T.E., and Lieber, M.R. (1999). A role for FEN-1 in nonhomologous DNA end joining: the order of strand annealing and nucleolytic processing events. Proc Natl Acad Sci U S A *96*, 1303-1308.

8 Acknowledgements

First of all, I thank Prof. Ulrich Hübscher for giving me the opportunity to perform my thesis in his laboratory, for his excellent guidance and support during my entire working time.

Next I thank Prof. Hanspeter Nägeli for co-refereeing my thesis.

A special thank goes to Rebecca Buob and Barbara van Loon who thought me all the necessary working steps and supervised my entire work, always supporting and helping whenever help was needed.

Furthermore I wish to thank all my other working colleagues in the Institute of Veterinary Biochemistry and Molecular Biology for their ongoing help and support in any situation.

The continuous and lively discussions with the founder of the „metasystem PerZan" Karsten Knut Panzer is acknowledged.

Finally I thank my family, Iwan Steiner and all my other friends outside the laboratory for their moral support.

9 Curriculum vitae

First Name:	Céline
Last Name:	Clemenz
Date of birth:	July 30th, 1983
Place of birth:	Brig, Switzerland
Nationality:	Swiss
Heimatort:	Stalden-Staldenried, Switzerland

1990 - 1996	Primary school, Leuk-Stadt, Wallis
1996 - 1999	Orientierungsschule Region Leuk, Leuk-Stadt, Wallis
1999 - 2004	Kollegium Spiritus Sanctus, Brig, Wallis
2004 - today	Studies in Veterinary Medicine at the Vetsuisse Faculty, University of Zürich, Switzerland
2008-2009	Thesis work at the Institute of Veterinary Biochemistry and Molecular Biology in the context of the „Schwerpunktstudium”

Zürich, January 3th, 2009